Title
LEPTONIC DECAYS OF NEUTRAL K MESONS

Author
Golden, Robert Leon.

Publication Date
1966-03-28

UNIVERSITY OF CALIFORNIA
Lawrence Radiation Laboratory
Berkeley, California

AEC Contract No. W-7405-eng-48

LEPTONIC DECAYS OF NEUTRAL K MESONS

Robert Leon Golden

(Ph. D. Thesis)

March 28, 1966

LEPTONIC DECAYS OF NEUTRAL K MESONS

Contents

LEPTONIC DECAYS OF NEUTRAL K MESONS

Robert Leon Golden

Lawrence Radiation Laboratory
University of California
Berkeley, California

March 28, 1966

Abstract

In the Alvarez 72-inch hydrogen bubble chamber, neutral K mesons are obtained from 6544 reactions of the type $\pi^- p \rightarrow \Lambda K^0$, with a visible Λ decay, $\Lambda \rightarrow p\pi^-$ (the beam was operated at π^- momenta of 1035 and 1170 MeV/c). A sample of 54 neutral K decays of the types $K \rightarrow \pi^{\pm} e^{\mp} \nu$, $\pi^{\pm} \mu^{\mp} \nu$ is examined to test the $\Delta I = 1/2$ and $\Delta S = \Delta Q$ selection rules. An analysis of about one third of the 54-event sample has been previously published by Alexander et al. The long-lived K_L leptonic decay rate was measured and found to be $\Gamma_L = (11.3 \pm 1.9) \times 10^6$/sec. This differs by 0.6 standard deviation from the $\Delta I = 1/2$ prediction $\Gamma_L = 2 [\Gamma(K^+_{e3}) + \Gamma(K^+_{\mu 3})] = (12.4 \pm 0.7) \times 10^6$/sec. We use 31 events for which the lepton charge is known to construct a likelihood function based on the T-invariant time distribution $1 + \gamma \exp(-\lambda_s t) + 2q\alpha \cos \Delta m t \exp(-\lambda_s t/2)$, where $q = +1$ if the decay involves a positive lepton and $q = -1$, if the decay involves a negative lepton. Using $\Delta m = 0.75 \times 10^{10}$/sec, we measure $\gamma = 1.4^{+1.4}_{-0.9}$, $\alpha = 1.0^{+0.3}_{-0.5}$, consistent with the $\Delta S = + \Delta Q$ predictions $\gamma = 1.0$, $\alpha = 1.0$. We also present an analysis of the time distribution of all 54 events. The time distribution used was $1 + Z \exp(-\lambda_s t) - 2\beta \exp(-\lambda_s t/2) \sin \Delta m t$. Assuming $\Delta m = 0.75 \times 10^{10}$/sec, we find $Z = -0.7^{+1.2}_{-0.8}$, $\beta = -0.8^{+0.5}_{-0.7}$. The $\Delta S = \Delta Q$ rule prediction is $Z = 1 + 0.6$, $\beta = 0$; the 0.6 is a correction for the $K_s \rightarrow \pi^+ \pi^- \gamma$ process. The likelihood of the $\Delta S = \Delta Q$ prediction is less the maximum by $e^{-0.6}$. T symmetry requires $\beta = 0$. Our results are consistent with T symmetry, but we cannot rule out significant T-nonpreserving amplitudes.

I. Introduction

By examining in the Alvarez 72-inch hydrogen bubble chamber 6544 reactions of the type $\pi^- p \rightarrow \Lambda K^0$ followed by a visible Λ decay $\Lambda \rightarrow p\pi^-$, we have found $\approx$ 2500 normal K decays ($K \rightarrow \pi^+\pi^-$) and 54 decays of the type $K \rightarrow \pi^{\pm} e^{\mp} \nu$ or $\pi^{\pm}\mu^{\mp}\nu$. About one-third of these events have been previously published by Alexander et al.[1] We use the 54 decays to measure the leptonic decay rate of the long-lived neutral K; this provides a test of the $\Delta I = 1/2$ rule for leptonic decays. We analyze the time distribution of the 54 decays with the intent of testing time-reversal symmetry and the $\Delta S = \Delta Q$ rule. We also analyze the time distribution of the 31 events in which the charged lepton is unambiguously identified.

We begin with an introduction to the neutral K system.

The K^0-$\overline{K}^0$ system is a most unusual one. Strangeness-mixing weak interactions allow K^0 to change to $\overline{K}^0$ and vice versa. This leads to the unusual situation wherein the eigenstates of strong interactions (K^0 and $\overline{K}^0$) are not eigenstates of the Hamiltonian for the isolated neutral K system (the eigenstates for the isolated system are called K_S and K_L).

One of the best qualitative pictures of the time development of an isolated neutral K particle is given by the pendulum analogy of Crawford.[2] The analogy stems from picturing the K^0 and $\overline{K}^0$ as two weakly coupled harmonic systems. This could be simulated in a number of ways. For example two coupled tank circuits could be used. The use of two weakly coupled pendulums is particularily satisfying because it gives one something quite tangible to play with.

The coupled pendulum is treated in many mechanics texts.[3] We will review here the general properties of the system. Consider two

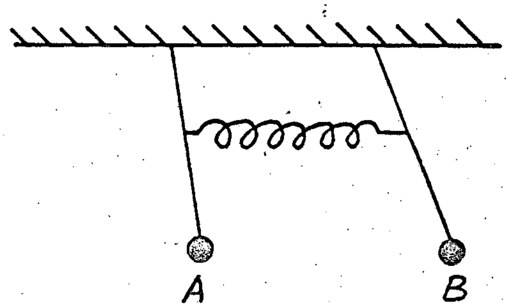

pendulums of equal period coupled by a weak spring. The system has two normal modes: 1, A and B move 180 deg out of phase: i.e., $v_A = v_0 \cos\omega_1 t$, $v_B = -v_0 \cos\omega_1 t$; 2, A and B move in phase, $v_A = v_0 \cos\omega_2 t$, $v_B = v_0 \cos\omega_2 t$. The frequencies of the modes are close together if the coupling is weak. Perhaps the most striking characteristic of the system is the periodic energy transfer. If A is started in motion while B is stationary, the flexing of the spring will eventually transfer all of A's energy to B and A will be stationary. Then the reverse takes place; the spring transfers B's energy to A. In the absence of damping the energy will continue to shuttle back and forth. If, however, damping is added in the form of friction losses in the spring, normal mode 1 will be damped out. Figure 1 displays the time dependence of the energies of A and B when the damping time is equal to the frequency difference of the normal modes.

To relate this system to the K^0 - $\overline{K}^0$ system, associate the energy of A with the intensity of K^0, and associate B with the $\overline{K}^0$. Normal mode 1 represents the K_S eigenstate, wherein the flexing of the spring represents the $\pi\pi$ virtual states, and the damping of the spring represents $\pi\pi$ decays. Mode 2 is the long-lived K_L. Starting with a K^0 at time zero is just like starting with A in motion and B stationary. The damping time is just the lifetime of the K_S (λ_S), and the difference in normal-mode frequency is the K_S-K_L mass difference. Figure 1 gives a qualitative picture of the amounts of K^0 and $\overline{K}^0$ as a function of time. For K^0 produced with a momentum of 500 MeV/c the predominance of $\overline{K}^0$ occurs roughly 6 cm away from the production. This indeed has been observed.[4]

As we shall see in the Theory section, the $\Delta S = \Delta Q$ rule says that $\pi^- e^+ \nu$ and $\pi^- \mu^+ \nu$ decays come from K^0 (and not from $\overline{K}^0$), also $\pi^+ e^- \nu$ and $\pi^+ \mu^- \nu$ come from $\overline{K}^0$ (and not from K^0). So if the $\Delta S = \Delta Q$ rule is valid, $\pi^- e^+ \nu$ and $\pi^- \mu^+ \nu$ indicate the presence of K^0 and thus these decay modes should be distributed as Fig. 1a (if we have pure K^0 at time zero). Similarly the $\Delta S = \Delta Q$ rule indicates that $\pi^+ e^- \nu$ and $\pi^+ \mu^- \nu$ decays should be distributed as Fig. 1b. To get a quantitative measure of the amount of $\Delta S = \Delta Q$ violation (if any)

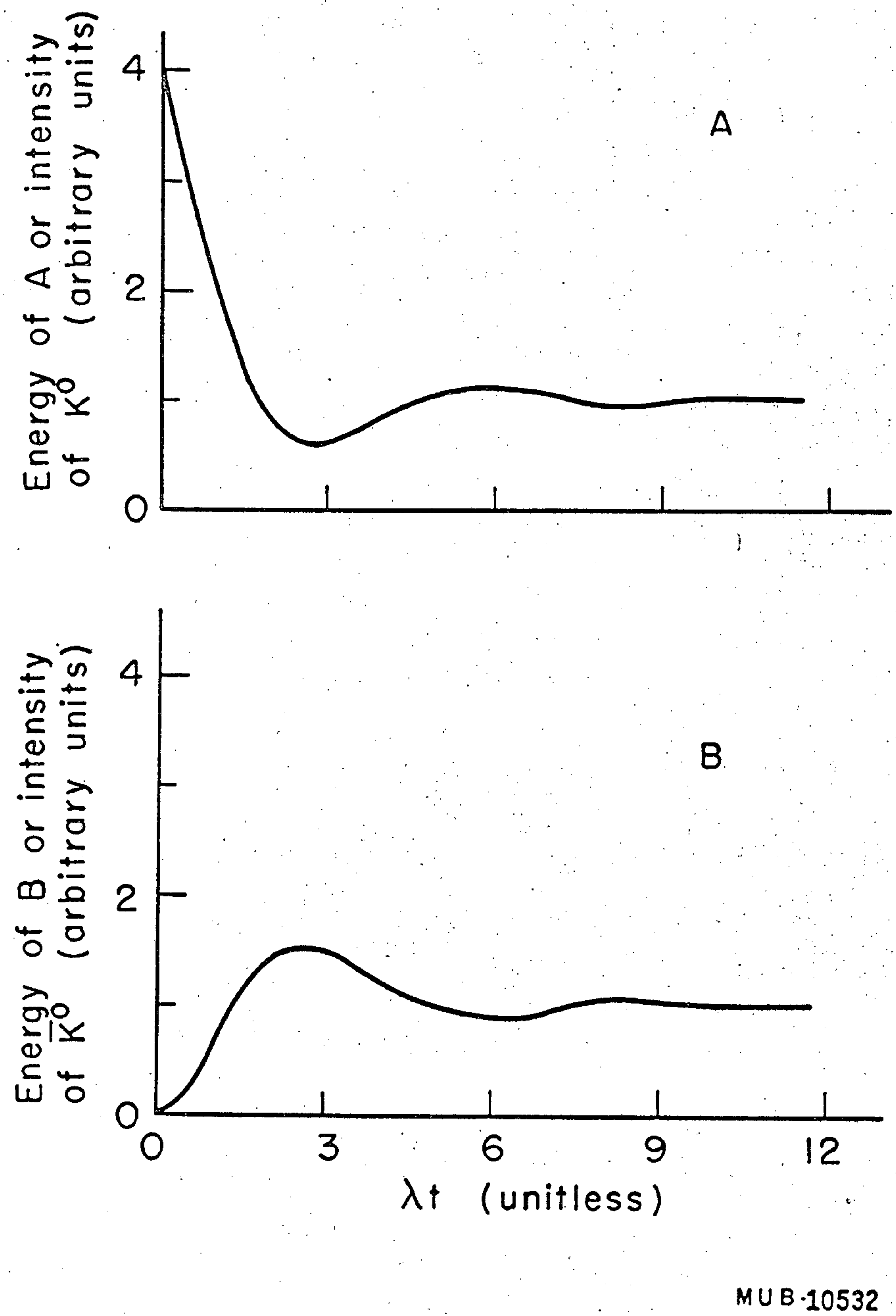

Fig. 1. The time dependence of a coupled pendulum.

one calculates the time distributions, allowing both $\Delta S = +\Delta Q$ and $\Delta S = -\Delta Q$ amplitudes. This is done in the Theory section.

The experimental tests of the $\Delta S = \Delta Q$ rule[1, 5-9] give somewhat contradictory results. The experiment is difficult to perform because the decay rate for $K_S \rightarrow \pi^+\pi^-$ is quite large compared with the leptonic decay rates. One of the backgrounds we have to deal with is from the process $K_S \rightarrow \pi^+\pi^-\gamma$. This decay is often kinematically ambiguous with a $\pi\mu\nu$ decay because of measurement inaccuracies. In our experiment almost any $\pi\mu\nu$ will also fit $\pi\pi\gamma$, and some $\pi\pi\gamma$ decays will fit $\pi\mu\nu$. The rate for $\pi\pi\gamma$ decay has been calculated on the assumption that is is entirely due to electromagnetic final-state interactions of a $K_S \rightarrow \pi^+\pi^-$ decay (the validity of this assumption is discussed in the Analysis section). In the Experimental Procedure section we present a technique of partially eliminating the background, and in the Analysis section we present a method for correcting for the remaining $\pi\pi\gamma$ background. Since the $\pi\pi\gamma$ decays should be distributed in time as are the K_S, their inclusion in the leptonic-decay time distribution would have the effect of enhancing the K_S leptonic decay rate. The ratio of the K_S leptonic-decay rate to the K_L leptonic decay rate (Γ_S/Γ_L) is predicted by the $\Delta S = \Delta Q$ rule to be 1.0. Thus the presence of a $\pi\pi\gamma$ background would lead to larger values of Γ_S/Γ_L and an apparent violation of the $\Delta S = \Delta Q$ rule. Note that if we use only the 31 events in which the charged lepton is unambiguously identified, there is no $\pi\pi\gamma$ background; in addition, these events are more sensitive to violations of the $\Delta S = \Delta Q$ rule than the events in which the lepton has not been identified.

The tests of the $\Delta S = \Delta Q$ rule which we will be using all depend on the time distributions of events in the first few K_S mean lives. We have 22 events with times less than 5×10^{-10} sec (about 5.5 K_S mean lives), thus the statistics available for testing the $\Delta S = \Delta Q$ rule are quite limited. Although we find no disagreement with the $\Delta S = \Delta Q$ rule, we cannot rule out $\Delta S = -\Delta Q$ amplitudes of the same size as the $\Delta S = \Delta Q$ amplitudes.

The time distributions of the leptonic decays also contain information about time-reversal symmetry. This is discussed in the Theory section. Again, the tests of time-reversal symmetry depend on the data in the first few K_S mean lives. We find no evidence for a violation of time-reversal symmetry, but we cannot rule out amplitudes that significantly fail to preserve T (time reversal).

The $\Delta I = 1/2$ rule can be used to relate the total leptonic decay rate of the K_L (Γ_L) to the three-body leptonic decay rate of the K^+ [$\Gamma_+ \equiv \Gamma(K^+_{e3}) + \Gamma(K^+_{\mu 3})$]. The relation is simply $\Gamma_L = 2\Gamma_+$; this relation is derived in the Theory section. The value of Γ_L has been measured by Alexander et al.[1] as $(9.31 \pm 2.49) \times 10^6$/sec, and by Franzini et al.[9] as $(9.4 \pm 1.3) \times 10^6$/sec. The value given by Alexander et al. was 2.6 standard deviations less than the prediction $\Gamma_L = 2\Gamma_+ = (16.5 \pm 1.2) \times 10^6$/sec [obtained by using the then current result $\Gamma_+ = (8.25 \pm 0.6) \times 10^6$/sec]. Later K^+-decay results give $\Gamma_+ = (6.2 \pm 0.35) \times 10^6$/sec,[10] which reduces the discrepancy between the result of Alexander et al. and the $\Delta I = 1/2$ prediction to 1.2 standard deviations. Franzini et al. found $\Gamma_L/\Gamma_+ = 1.7 \pm 0.3$, assuming $\Delta S = \Delta Q$ and using $\Gamma_+ = (6.2 \pm 0.8) \times 10^6$/sec. This value is 1 standard deviation less than the $\Delta I = 1/2$ prediction. After checking for internal consistency, we combine the events of Alexander et al. and the new events to find $\Gamma_L = (11.3 \pm 1.9) \times 10^6$/sec, which is 0.6 standard deviation less than the $\Delta I = 1/2$ prediction.

II. Theory

A. The Time Distribution of Leptonic Decays

The objective in this section is to calculate the time distribution for leptonic decays in terms of the $\Delta S = \Delta Q$ and $\Delta S = -\Delta Q$ decay amplitudes.

In the reaction $\pi^- p \rightarrow \Lambda K^0$ we have, initially, a pure K^0 wave function. We'll define the moment of production to be $t = 0$. All times mentioned subsequently will refer to time in the rest frame of the K^0. As time develops, the strangeness-mixing weak interactions allow the K^0 to change to a $\overline{K}^0$. In general, then, the K^0 and $\overline{K}^0$ are not eigenstates of the Hamiltonian for an isolated neutral K particle. Neglecting the CP-nonpreserving part of the eigenstates, we have, to an accuracy of $\approx 1/500$,[11, 12]

$$|K_S\rangle = \frac{|K^0\rangle + |\overline{K}^0\rangle}{\sqrt{2}} \quad \text{(the short-lived component)},$$
$$|K_L\rangle = \frac{|K^0\rangle - |\overline{K}^0\rangle}{\sqrt{2}} \quad \text{(the long-lived component)}. \tag{1}$$

The time dependence of the eigenstates is given by the Weiskopf-Wigner form,[13]

$$|K_S(t)\rangle = |K_S(0)\rangle \exp-(\lambda_S/2 + im_S)t \equiv |K_S(0)\rangle\, f_S(t),$$
$$|K_L(t)\rangle = |K_L(0)\rangle \exp-(\lambda_S/2 + im_L)t \equiv |K_L(0)\rangle\, f_L(t), \tag{2}$$

where m_S and m_L are the masses of the short- and long-lived components (in units such that $\hbar = c = 1$), and the parameters λ_S and λ_L are the total decay rates of the K_S and K_L, respectively.

At time zero we have $|K^0\rangle = \dfrac{|K_S\rangle + |K_L\rangle}{\sqrt{2}}$; this state evolves with respect to time, becoming a different superposition of K_S and K_L at time t,

$$\Psi(t) = \frac{1}{\sqrt{2}}\left[|K_S(0)\rangle f_S(t) + |K_L(0)\rangle f_L(t)\right]. \tag{3}$$

We can rewrite the state in terms of the K^0 and $\overline{K}^0$:

$$\Psi(t) = \frac{1}{2}\left[|K^0\rangle (f_S(t) + f_L(t)) + |\overline{K}^0\rangle (f_S(t) - f_L(t))\right]. \tag{4}$$

Now we define amplitudes for the leptonic-decay processes

$$K^0 \rightarrow \pi^- l^+ \nu \quad \text{(amplitude } a_+\text{)}, \tag{5}$$
$$K^0 \rightarrow \pi^+ l^- \nu \quad \text{(amplitude } a_-\text{)},$$

where l can stand for electron or muon. Note that a_+ and a_- both may depend on spins and momenta. The amplitudes for the analogous $\overline{K}^0$ processes can be related to a_+ and a_- by use of the CPT theorem (the calculation is performed in Appendix A):

$$\overline{K}^0 \rightarrow \pi^+ l^- \nu \quad \text{(amplitude } a_+^*\text{)},$$
$$\overline{K}^0 \rightarrow \pi^- l^+ \nu \quad \text{(amplitude } a_-^*\text{)}. \tag{6}$$

The amplitude for l^+ decay with momenta and spins $\underset{\sim}{p}_i$, $\underset{\sim}{\sigma}_i$ is

$$a(\underset{\sim}{p}_i, \underset{\sim}{\sigma}_i, l^+, t) = a_+ \langle K^0 | \Psi(t) \rangle + a_-^* \langle \overline{K}^0 | \Psi(t) \rangle . \tag{7}$$

Using Eqs. (4) and (7) we find

$$a(\underset{\sim}{p}_i, \underset{\sim}{\sigma}_i, l^+, t) = \frac{1}{2} [a_+ (f_S(t) + f_L(t)) + a_-^* (f_S(t) - f_L(t))] . \tag{8}$$

Squaring Eq. (8) and neglecting $\lambda_L t$ (which is always small for our events) gives the intensity (at time t) of l^+ decays with a given set of momenta and spins. Averaging over momenta and spins, adding e^+ and μ^+ decay intensities, and normalizing to N_0 neutral K's at time zero gives

$$\frac{dN}{dt}(+, t) = \frac{N_0}{4} \Bigg[\sum_l \langle |a_+ - a_-^*|^2 \rangle + \exp(-\lambda_S t) \sum_l \langle |a_+ + a_-^*|^2 \rangle$$
$$+ 2 \exp(-\lambda_S t/2) \cos\Delta m t \sum_l \langle \mathrm{Re}(a_+ - a_-^*)(a_+ + a_-^*) \rangle$$
$$- 2 \exp(-\lambda_S t/2) \sin\Delta m t \sum_l \langle \mathrm{Im}(a_+ - a_-^*)(a_+ + a_-^*) \rangle \Bigg] , \tag{9}$$

where $\Delta m = m_S - m_L$,

$\sum_l$ = sum over e and μ,

$\langle \; \rangle$ = average over momenta and spins.

The term $\sum_{l} \langle |a_+ - a_-^*|^2 \rangle$ is the total K_L leptonic decay rate (Γ_L), and the term $\sum_{l} \langle |a_+ + a_-^*|^2 \rangle$ is the total K_S leptonic decay rate (Γ_S). This can be seen by calculating the decay rate of a state that is pure K_S or K_L at time zero.

Equation (9) can be rewritten as

$$\frac{dN}{dt}(+,t) = \frac{N_0 \Gamma_L}{4} [1 + \gamma \exp(-\lambda_S t) + 2 \exp(-\lambda_S t/2) \times (\alpha \cos \Delta mt - \beta \sin \Delta mt)] , \qquad (10)$$

where

$$\gamma = \frac{\sum_{l} \langle |a_+ + a_-^*|^2 \rangle}{\sum_{l} \langle |a_+ - a_-^*|^2 \rangle} = \frac{\Gamma_S}{\Gamma_L}$$

$$\alpha = \frac{\sum_{l} \langle \mathrm{Re}(a_+ + a_-^*)(a_+ - a_-^*) \rangle}{\sum_{l} \langle |a_+ - a_-^*|^2 \rangle}$$

$$\beta = \frac{\sum_{l} \langle \mathrm{Im}(a_+ + a_-^*)(a_+ - a_-^*) \rangle}{\sum_{l} \langle |a_+ - a_-^*|^2 \rangle} .$$

To calculate $\frac{dN}{dt}(-,t)$, just interchange a_+ and a_- in Eq. (9). The result is that the α term in Eq. (10) changes sign. The general formula is then

$$\frac{dN}{dt}(\pm,t) = \frac{N_0 \Gamma_L}{4} [1 + \gamma \exp(-\lambda_S t) + 2 \exp(-\lambda_S t/2) \times (\pm \alpha \cos \Delta mt - \beta \sin \Delta mt)] . \qquad (11)$$

If we do not make use of the lepton charge information, the (+) and (-) intensities can be added. The α term drops out, leaving,

$$\frac{dN}{dt}(t) = \frac{N_0 \Gamma_L}{2} [1 + \gamma \exp(-\lambda_S t) - 2\beta \exp(-\lambda_S t/2) \sin \Delta mt] . \qquad (12)$$

B. The $\Delta I = 1/2$ Rule

1. The $\Delta S = \Delta Q$ Rule

The $\Delta S = \Delta Q$ rule for leptonic decays of strange particles is that the change in strangeness of the strong particles in a decay equals the change in charge (in units of e) of the strong particles in the decay (i.e., $\Delta S = \Delta Q$). As an example, consider the decay $K^0 \to \pi^+ e^- \nu$. The strangeness of the strong particle in the initial state is +1, and the strangeness of the strong particle in the final state is zero, so $\Delta S = -1$. The charge of the strong particle in the initial state is zero, and in the final state the charge of the strong particle is +1, thus $\Delta Q = +1$. So for $K^0 \to \pi^+ e^- \nu$ one has $\Delta S = -\Delta Q$, which is forbidden by the $\Delta S = \Delta Q$ rule. Of the decays studied in this experiment,

$$K^0 \to \pi^- e^+ \nu,\ \pi^- \mu^+ \nu \quad \text{(amplitude } a_+)$$

and $$\overline{K}^0 \to \pi^+ e^- \nu,\ \pi^+ \mu^- \nu \quad \text{(amplitude } a_+^*)$$

are allowed by the $\Delta S = \Delta Q$ rule, and

$$K^0 \to \pi^+ e^- \nu,\ \pi^+ \mu^- \nu \quad \text{(amplitude } a_-)$$

and $$\overline{K}^0 \to \pi^- e^+ \nu,\ \pi^- \mu^+ \nu \quad \text{(amplitude } a_-^*)$$

are forbidden.

It is interesting to note that the $\Delta S = \Delta Q$ rule is a consequence of the $\Delta I = 1/2$ rule. The $\Delta I = 1/2$ rule for leptonic decays is that the I spin of the initial-state and the I spin of the final state differ by an isospinor (i.e., $|\Delta I, \Delta I_z\rangle = |1/2, 1/2\rangle$ or $|1/2 -1/2\rangle$). The I spin of the final state is calculated by combining the I spins of <u>only the strongly interacting particles</u> in the final state. Now consider the reaction $K^0 \to \pi^+ e^- \nu$. The initial I spin is $|1/2. -1/2\rangle$ and the final-state I spin is $|1, 1\rangle$ (remember it is the I spin of the strong particle only), therefore ΔI must be 3/2. Thus the $\Delta I = 1/2$ rule forbids the reaction $K^0 \to \pi^+ e^- \nu$. This decay is also forbidden by the $\Delta S = \Delta Q$ rule. By similar analysis, it can be found that the $\Delta I = 1/2$ rule gives the same forbidden and allowed reactions as the $\Delta S = \Delta Q$ rule. Thus the $\Delta S = \Delta Q$ rule can be thought of as a consequence of the $\Delta I = 1/2$ rule. Our proof was only for leptonic decays; a much more general proof can be found in Ref. 14.

Note that amplitude a_- is responsible for the forbidden reactions. Thus the $\Delta S = \Delta Q$ rule requires $a_- = 0$. Consequently the $\Delta S = \Delta Q$ rule implies that the time distribution of leptonic decays should obey Eq. (11) with $\alpha = \gamma = 1$, $\beta = 0$ or Eq. (12) with $\gamma = 1$, $\beta = 0$.

2. Decay Rates

The $\Delta I = 1/2$ rule can be used to relate decay rates of K_L and K^+. Rewrite the reaction $K^+ \rightarrow \pi^0 e^+ \nu$ as $\pi^0 K^+ \rightarrow e^+ \nu$. Now we'll use the spurion formalism of Wentzel[15]. The reaction is regarded as $\pi^0 K^+ \rightarrow S$, where S is a spurion; it carries away the I spinor. The reaction amplitude is supposed to be independent of I (I spin) and it is supposed to conserve I. To begin, we write out the state $\pi^0 K^+$ in terms of I spin vectors, using the Clebsch-Gordan tables,

$$\pi^0 K^+ = |1, 0\rangle_\pi \otimes |\tfrac{1}{2}\ \tfrac{1}{2}\rangle_K = \sqrt{\tfrac{2}{3}}\ |\tfrac{3}{2}\ \tfrac{1}{2}\rangle_{\pi K} - \sqrt{\tfrac{1}{3}}\ |\tfrac{1}{2}\ \tfrac{1}{2}\rangle_{\pi K} . \quad (13)$$

Thinking in terms of perturbation theory, we calculate $\Gamma(K^+ \rightarrow \pi^0 e^+ \nu)$ in terms of

$$\langle S|H|\pi^0 K^+\rangle = \sqrt{\tfrac{2}{3}}\ \langle S|H|\tfrac{3}{2}\ \tfrac{1}{2}\rangle_{\pi K} - \sqrt{\tfrac{1}{3}}\ \langle S|H|\tfrac{1}{2}\ \tfrac{1}{2}\rangle_{\pi K} . \quad (14)$$

The $\Delta I = 1/2$ rule says that the $I = 3/2$ term is zero. Using Fermi's Golden Rule, we have

$$\Gamma(K^+ \rightarrow \pi^0 e^+ \nu) = \frac{2\pi}{\hbar} \cdot \frac{1}{3} \cdot |\langle S|H|\tfrac{1}{2}\ \tfrac{1}{2}\rangle_{\pi K}|^2\ \rho(K^+ \rightarrow \pi^0 e^+ \nu), \quad (15)$$

where ρ is the available phase space for the reaction. Now we calculate the K_L decay rates in terms of spurion matrix elements:

$$|K_L\rangle = \frac{1}{\sqrt{2}}\,[\,|K^0\rangle - |\bar{K}^0\rangle\,] . \quad (16)$$

For $K_L \rightarrow \pi^+ e^- \nu$, rewrite the reaction as $\pi^- K_L \rightarrow S$. Then, using Eq. (16), we can write

$$\langle S|H|K_L\rangle = \frac{1}{\sqrt{2}}\,[\,\langle S|H|\pi^- K^0\rangle - \langle S|H|\pi^- \bar{K}^0\rangle\,] . \quad (17)$$

Using the same technique as above, and setting the $\frac{3}{2}$ terms to zero, we calculate the $\pi^- K^0$ matrix element,

$$\langle S|H|\pi^- K^0\rangle = \langle S|H|\,[\,|1\,-1\rangle_\pi \otimes |\tfrac{1}{2}\,-\tfrac{1}{2}\rangle_K\,]$$

$$= \langle S|H|\,\tfrac{3}{2}\,-\tfrac{3}{2}\rangle_{\pi K} = 0, \tag{18}$$

and, similarily,

$$\langle S|H|\pi^- \bar{K}^0\rangle = \langle S|H|[\,|1\,-1\rangle_\pi \otimes |\tfrac{1}{2}\,\tfrac{1}{2}\rangle_K]\,.$$

$$= \langle S|H|(-\sqrt{\tfrac{1}{3}}\,|\tfrac{3}{2}\,-\tfrac{1}{2}\rangle_{\pi K} + \sqrt{\tfrac{2}{3}}\,|\tfrac{1}{2}\,-\tfrac{1}{2}\rangle_{\pi K})$$

$$= \sqrt{\tfrac{2}{3}}\,\langle S|H|\tfrac{1}{2}\,-\tfrac{1}{2}\rangle_{\pi K}\,. \tag{19}$$

So,

$$\langle S|H|\pi^- K_L\rangle = \frac{-1}{\sqrt{2}}\cdot\sqrt{\frac{2}{3}}\,\langle S|H|\tfrac{1}{2}\,-\tfrac{1}{2}\rangle_{\pi K}$$

$$= -\sqrt{\tfrac{1}{3}}\,\langle S|H|\tfrac{1}{2}\,-\tfrac{1}{2}\rangle_{\pi K}\,. \tag{20}$$

Using Eq. (20) and the Golden Rule, one finds the rate for $K \to \pi^- e^+ \nu$ is

$$\Gamma(K_L \to \pi^- e^+ \nu) = \frac{2\pi}{\hbar}\cdot\frac{1}{3}\cdot\left|\langle S|H|\tfrac{1}{2}\,-\tfrac{1}{2}\rangle_{\pi K}\right|^2 \rho(K_L \to \pi^- e^+ \nu). \tag{21}$$

The phase-space factor $\rho(K_L \to \pi^- e^+ \nu)$ is very nearly equal to $\rho(K^+ \to \pi^0 e^+ \nu)$, so we'll write the above equation as

$$\Gamma(K_L \to \pi^- e^+ \nu) = \frac{2\pi}{\hbar}\cdot\frac{1}{3}\cdot\left|\langle S|H|\tfrac{1}{2}\,-\tfrac{1}{2}\rangle_{\pi K}\right|^2 \rho(K^+ \to \pi^0 e^+ \nu). \tag{22}$$

By calculations similar to those above, one finds

$$\Gamma(K_L \to \pi^+ e^- \nu) = \frac{2\pi}{\hbar}\cdot\frac{1}{3}\cdot\left|\langle S|H|\tfrac{1}{2}\,\tfrac{1}{2}\rangle_{\pi K}\right|^2 \rho(K^+ \to \pi^0 e^+ \nu). \tag{23}$$

In order to add the $\pi^+ e^- \nu$ and $\pi^- e^+ \nu$ rates, we note that the squares of the matrix elements are equal because the states differ only by a rotation in I-spin space:

$$\left|\langle S|H|\tfrac{1}{2}\,-\tfrac{1}{2}\rangle_{\pi K}\right|^2 = \left|\langle S|H|\tfrac{1}{2}\,\tfrac{1}{2}\rangle_{\pi K}\right|^2. \tag{24}$$

Therefore combining rates for $\pi^+ e^- \nu$ and $\pi^- e^+ \nu$ gives

$$\Gamma(K_L \to \pi^\pm e^\mp \nu) = \frac{2\pi}{\hbar}\cdot\frac{2}{3}\cdot\left|\langle S|H|\tfrac{1}{2}\,\tfrac{1}{2}\rangle_{\pi K}\right|^2 \rho(K^+ \to \pi^0 e^+ \nu). \tag{25}$$

Thus, using Eq. (15) and (25), we have

$$\frac{\Gamma(K^+ \to \pi^0 e^+ \nu)}{\Gamma(K_L \to \pi^\pm e^\mp \nu)} = \frac{1}{2} . \tag{26}$$

By an almost identical derivation, the same result holds for decays involving a muon instead of an electron. Thus

$$\frac{\Gamma_+ \equiv \Gamma(K^+ \to \pi^0 e^+ \nu) + \Gamma(K^+ \to \pi^0 \mu^+ \nu)}{\Gamma_L \equiv \Gamma(K_L \to \pi^\pm e^\mp \nu) + \Gamma(K_L \to \pi^\pm \mu^\mp \nu)} = \frac{1}{2} . \tag{27}$$

C. The meaning of β

A nonzero value of β is an indication of nonpreservation of time-reversal symmetry. As shown in Appendix A, time-reversal invariance implies that a_+ and a_- are real. Thus, since β is proportional to $\text{Im}(a_+ - a_-^*)(a_+ + a_-^*)$, time-reversal invariance implies $\beta = 0$.

Sachs has presented a theory which explains the T-nonconserving K decays in terms of nonconservation of T in the leptonic decay channels.[16] His theory requires that a_+ and a_- have roughly the same magnitude and that their ratio be predominantly imaginary. The relationship between a_+ and a_- which gives the largest T asymmetry in K_L decays is $a_+/a_- = \pm i$. We will refer to this case as the Sachs limit. In this limit $\gamma = 1$, $\alpha = 0$ and $\beta = \pm 1$.

D. Summary

In the previous three sections we have seen that, if the lepton charge information is available, we can use the time distribution of the leptonic decays given by

$$\frac{dN}{dt} = \frac{N_0 \Gamma_L}{4} [1 + \gamma \exp(-\lambda_S t) + 2 \exp(-\lambda_S t/2)(\pm \alpha \cos \Delta mt - \beta \sin \Delta mt)] , \tag{11}$$

where $(\pm)$ stands for the sign of the charge of the charged lepton in the decay. If the lepton charge information is not available, we can use

$$\frac{dN}{dt} = \frac{N_0 \Gamma_L}{2} [1 + \gamma \exp(-\lambda_S t) - 2\beta \exp(-\lambda_S t/2) \sin \Delta mt] . \tag{12}$$

The values of α, β, and γ in the above equations are predicted by the $\Delta S = \Delta Q$ rule to be 1, 0, and 1 respectively. Any nonzero value of β is an indication of an asymmetry with respect to T. We have also found that the $\Delta I = 1/2$ rule relates the K_L and the K^+ three-body leptonic decay rates by $\Gamma_L = 2\Gamma_+$.

We will now turn to the matter of acquiring a sample of leptonic decays of the K in order to measure α, β, γ, and Γ_L.

III. Experimental Procedures

A. The Beam

The π^- beam system was designed and built by Professor Frank S. Crawford, Jr.[17] It was used in conjunction with the Alvarez 72-inch hydrogen bubble chamber during the fall of 1960 and the spring of 1961. Since the beam has been previously described, we give only a brief survey. A schematic diagram of the beam optics is given in Fig. 2. The most important single characteristic of the beam is very good momentum resolution. The full width at half maximum of the momentum distribution is $\approx$ 10 MeV/c. The run was made at π^- momenta of 1035 and 1170 MeV/c.

At 1035 MeV/c there are $\approx$ 150 000 pictures containing the events reported by Alexander et al.[1] and $\approx$ 120 000 pictures taken later in the run. The bubble chamber magnetic field was 13.5 kG for the 1035-MeV/c film. There are also $\approx$ 100 000 pictures taken at 1170 MeV/c, at which the magnetic field was 17.9 kG.

B. Procurement of the Candidates

We have included the events found by Alexander et al. in our analysis. In addition to these events we found 34 more. The selection process described below is the process used for the new events. The events of Alexander et al. were treated in a very similar manner. The major differences are noted in the text.

1. Scanning

The film was scanned for the decays of neutral strange particles and their associated productions. The reactions possible are

$$\pi^- p \rightarrow \Lambda K,$$

$$\pi^- p \rightarrow \Sigma^0 K, \Sigma^0 \rightarrow \Lambda\gamma .$$

These reactions appear in the bubble chamber as a terminating track

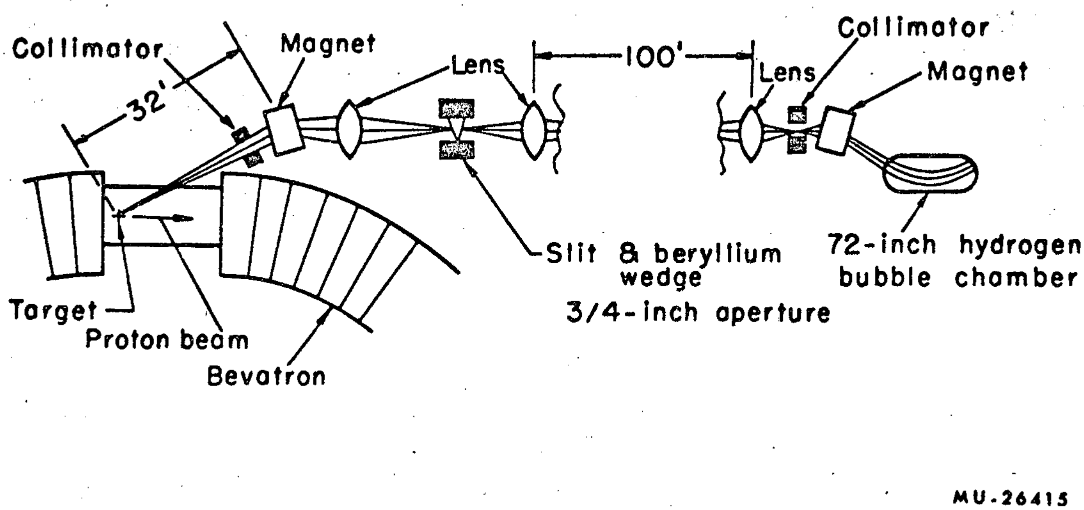

Fig. 2. Schematic diagram of the beam optics.

followed by one or two vees (we select the reaction $\pi p \rightarrow \Lambda K$ after the events are measured).

The Scanners were asked to record all events of these topologies except when

(a) The incident track is nonbeam, i. e., obviously differing in angle and momenta from the other beam tracks;

(b) the incident track has a previous interaction;

(c) too many tracks are found in the frame for accurate scanning (usually 30 or more); or

(d) no neutral track is longer than 3 mm on the scan table (4.5 mm true space). This criterion eliminates confusion with events in which no neutral track is involved (e.g., $\pi^- p \rightarrow \pi^- p$).

The scanning efficiencies (found by second scanning) are better than 95% for either topology.

The single-vee Λ events were rescanned for associated K decays missed during the first scan. The rescan was done with the benefit of a computed direction for the K decay (the events were all measured before rescan). The scanners were asked to record all possible decays within 5 degrees of the K^0 line of flight. We believe we have found 100% of the K decays, leptonic or not, associated with the Λ decays in our sample.

2. Measurement and Kinematic Analysis

The events were measured on the "Franckenstein" measuring projector and processed through the Alvarez Group PANAL-PACKAGE-EPC program system.[18]

The PACKAGE part of the program system performs spatial reconstruction of the measurement and makes least-squares fits to momentum- and energy-conservation equations according to hypotheses described below.

3. Selection of the Candidates

Any events that fit the hypotheses ($\Lambda \to p\pi^-$, $K \to \pi^+\pi^-$, $\pi^- p \to \Lambda K$) or ($\Lambda \to \pi^- p$, $K \to \pi^+\pi^-$, $\pi^- p \to \Sigma^0 K^0$) with $\chi^2 < 25$ for each fit are accepted as "normal" events and removed from consideration as lepton candidates. The remaining events are tried as $\Lambda \to p\pi^-$ followed by a three-constraint fit ($\pi^- p \to \Lambda K$) including information from the two-point track of the K; those that fit with each $\chi^2 < 25$ are accepted as lepton candidates. Events that have Σ^0-K^0 production generally do not meet this requirement. It should be mentioned that the Λ decay is almost always identifiable by the heavily ionizing decay proton; when there is any possible doubt, both vees are tried as $\Lambda \to p\pi$. The candidates are further reduced by requiring;

(a) That the decays be within a fiducial volume which is approximately 1 cm inside the visible part of the chamber. In the film used for the Alexander et al. events, there is also a maximum time for decays (20×10^{-10} sec).

(b) That the production be within a fiducial volume generally 1 cm inside the decay fiducial volume.

(c) That the Λ have a length greater than 8 mm. In the film used for Alexander et al. events, the Λ had to be longer than 5 mm; the K decays had to be more than 5 mm from the production vertex and occur more than 0.2×10^{-10} sec after the production.

C. Analysis of the Candidates

The candidates are required to pass the following tests:

(a) $K^0 \to \pi^+\pi^-$, where the π^+ or π^- undergoes an unseen scattering. We delete, one at a time, each of the charged tracks, and fit to the hypothesis $K^0 \to \pi^+\pi^-$, using the K momentum from the $\pi^- p \to \Lambda K$ fit. If the 1 c (i.e. one-constraint) χ^2 is less than 10 for either deleted track the decay could have been a normal $\pi^+\pi^-$ decay in which one of the pions has scattered. In order for the event to be removed from the candidate list, the deleted track of the event must further satisfy $p_{fit}\beta\Delta\theta < 2000$ MeV-deg/c, where p_{fit} is the momentum of the deleted track, β is its velocity, and $\Delta\theta$ is the space angle between the measured track and the track predicted by the fit. This condition is derived in Appendix B. We estimate that, out of 2500 K decays, less than 0.3 $K_1 \rightarrow \pi^+\pi^-$ with an associated Coulomb scattering would fail to be removed. This cutoff also removes $K_S \rightarrow \pi^+\pi^-$, where $\pi^\pm \rightarrow \mu^\pm \nu$. Of course, the tracks are also carefully examined for visible Coulomb scatterings, decays, and nuclear interactions.

(b) $K_S \rightarrow 2\pi^0, \pi^0 \rightarrow e^+e^-$. We assume that the charged tracks of the K-decay vertex are electrons and calculated their invariant mass. If $M(e^\pm)$ is less than 85 MeV, then the event is removed as a possible $e^\pm$. We expect ≈ 23 Dalitz pairs, and 99% of them should have $M(e^\pm)$ less than 85 MeV.[19]

(c) $K^0 \rightarrow \pi^+\pi^-\pi^0$. Using the K momentum from the production fit, we try the 1c hypothesis $K \rightarrow \pi^+\pi^-\pi^0$; if the χ^2 is less than 10.0, the event is accepted as a τ^0 decay (i.e., $K \rightarrow \pi^0\pi^+\pi^-$). The separation between τ^0 decays and leptonic decays is believed to be clean; no corrections are made. The τ^0 decays have been analyzed by Stern et al.[20]

(d) $K^0 p \rightarrow K_S p$ and $K_S \rightarrow \pi^+\pi^-$. We try the following set of consecutive hypotheses:

(i) $\Lambda \rightarrow p\pi^-$ (3c),

(ii) $\pi^- p \rightarrow \Lambda K_b$ (1c, without the two-point track of the K),

(iii) $K_c \rightarrow \pi^+\pi^-$ (1c, without the two-point track of the K),

(iv) $K_b p \rightarrow K_c p$ (1c).

The reaction (iv) means that a K-p scattering is tried with the momentum vectors from fits (ii) and (iii). If all the χ^2 are less than 10 and the proton recoil has a momentum less than 100 MeV/c, the event could be a K-p elastic scattering with an invisible recoil (followed by a normal decay). No candidates are removed by this cutoff.

In order to remove as much of the $\pi\pi\gamma$ background as possible, we take advantage of the expected predominance of the low-momentum γ rays.

(e) $K \rightarrow \pi^+\pi^-\gamma$. Again using the production fit to provide the K momentum, we try $K_S \rightarrow \pi^+\pi^-\gamma$. If the event is an unambiguous $\pi\pi\gamma$ decay, or if $\pi\pi\gamma$ fits and $p_\gamma < 70$ MeV/c, the event is removed from the candidates. Again, the criterion for a good fit of the K decay was χ^2 less than 10.[21]

Two of the events used by Alexander et al. were eliminated by this cutoff. The effects of the $\pi\pi\gamma$ decays that still survive this cutoff are discussed in the next section.

The surviving candidates all satisfy at least one 1c-lepton-hypothesis with $\chi^2 < 10$. The χ^2's for the events are listed in Table I. All the events were carefully examined to determine the charge of the lepton. The discussion of techniques for lepton-charge determination is contained in Appendix C.

As a verification that the decays which survive our selection criteria are predominantly leptonic decays, we present in Fig. 3 the χ^2 distribution of the K-decay vertex fitted to the 4c hypothesis $K_S \rightarrow \pi^+\pi^-$. Clearly the distribution is peaked at high χ^2 and gives no evidence of a tail from the normal events. To calculate the expected distribution, we simulated measurements of bona fide leptonic decays using program FAKE.[22] The events were generated according to V-A theory and were tried as $\pi^+\pi^-$ (4c).[23] The χ^2 distribution of electron-mode decays (normalized to 31 events) was added to the χ^2 distribution of the muon-mode decays (normalized to 23 events) to give the dashed histogram in Fig. 3.[24] The contribution of the expected 2.56 $\pi\pi\gamma$ decays was ignored in calculating the expected distribution. The two curves certainly have the same shape. In fact the degree of agreement, especially in the position of the peak, is somewhat surprising, since the generation process includes measurement-error estimates derived from completely independent experiments.

The selection process began with 6544 events of the type $\pi^-p \rightarrow \Lambda K^0$, $\Lambda \rightarrow p\pi^-$. Associated with these 6544 events were about 2500 decays along the K line of flight. Of the 2500 decays, 54 satisfy all the selection criteria and fit at least on leptonic hypothesis.

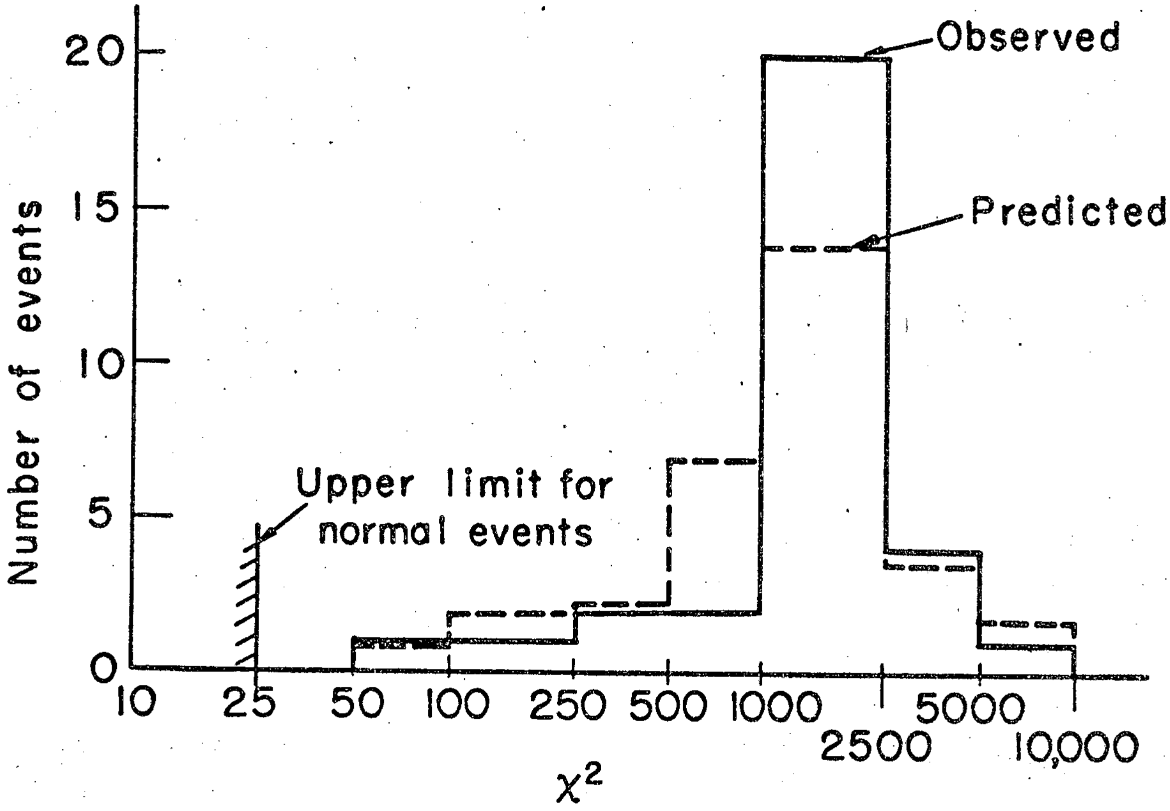

MUB-10533

Fig. 3. χ^2 Distribution of leptonic decays tried as normal two-body decays. Twenty-three events could not be fitted to the hypothesis $K \to \pi^+\pi^-$. This is because the iterative fitting procedure would not converge. The expected number of nonfitting events is 24.2.

IV. Analysis and Results

A. Use of Lepton Charge Information

In order to make use of the lepton charge information, a likelihood function was constructed on the basis of the time distribution in Eq. (11),

$$\mathcal{L}(\alpha,\beta,\gamma) = \prod_{31\ \text{events}} \frac{1+\gamma e^{-\lambda_S t_i}+2e^{-\lambda_S t_i/2}(q_i\,\alpha\cos\Delta m t_i-\beta\sin\Delta m t_i)}{\int_{h_i}^{w_i}[1+\gamma e^{-\lambda_S t}+2e^{-\lambda_S t/2}(q_i\,\alpha\cos\Delta m t-\beta\sin\Delta m t)]\,dt} \qquad (28)$$

where t_i = proper time of the decay;

q_i = sign of the charge of the charged lepton;

w_i = proper time to the edge of the fiducial region. This had an upper limit of 20×10^{-10} sec for the events of Alexander et al. (w stands for "wall" time);

h_i = minimum proper time for acceptance. This was zero for the new events. Alexander et al. used a cutoff of 0.2×10^{-10} sec or the time for the K to go 5 mm, whichever time was larger;

Δm = $K_S - K_L$ mass difference (in units of radians/sec). Meisner et al. combine six experiments to get $\Delta m = (0.64\pm0.06)\,\lambda_S = 0.77\times10^{10}$/sec for the world average.[3] We compute the likelihood $\mathcal{L}(\alpha,\beta,\gamma)$ assuming three values of Δm; $\Delta m = 0.6\times10^{10}$/sec, 0.75×10^{10}/sec, 0.9×10^{10}/sec.

The times for the events are given in Table I. It was found that unless we restricted $\beta\equiv0$, the likelihood was too broad to give any useful results. Making the constraint $\beta\equiv0$ (i.e., assuming T invariance), we calculated the likelihood function as a function of α,γ for three values of Δm:

Δm	α	γ
$0.54\ \lambda_S = 0.60\times 10^{10}/\text{sec}$	1.1	1.5
$0.66\ \lambda_S = 0.75\times 10^{10}/\text{sec}$	$1.0^{+0.3}_{-0.5}$	$1.4^{+1.4}_{-0.9}$
$0.79\ \lambda_S = 0.90\times 10^{10}/\text{sec}$	1.2	1.75

All the above values are quite consistent with the $\Delta S = \Delta Q$ prediction $\alpha = 1.0$, $\gamma = 1.0$. The contours of the likelihood function (when $\Delta m = 0.75\times 10^{10}/\text{sec}$ is used) are displayed in Fig. 4. Under the assumption $\beta \equiv 0.0$ the parameters γ and α are restricted, by unitarity, to satisfy $\gamma > \alpha^2$. This restriction is calculated in Appendix C.

We now turn to the analysis of all 54 events. Due to kinematic uncertainties this sample contains an estimated 2.56 $\pi\pi\gamma$ decays.

B. The $\pi\pi\gamma$ Correction

The rate for $K_S \to \pi^+\pi^-\gamma$ as a function of p_γ has been calculated independently by Beg, by Friedburg, and by Schultz. The calculation is made on the assumption that the process is entirely due to electromagnetic final-state interactions.[25] The differential decay rate is[26]

$$\frac{d\Gamma}{dp_\gamma} = \Gamma(K_S \to \pi^+\pi^-)\cdot\frac{\alpha}{\pi}\cdot\frac{dp_\gamma}{p_\gamma}\cdot\left(1-\frac{2p_\gamma}{m_K}\right)\cdot\frac{\beta}{\beta_{\pi\pi}}\cdot\left[\frac{1+\beta^2}{\beta}\ln\frac{1+\beta}{1-\beta} - 2\right] \quad (29)$$

where p_γ = photon momentum in the K_S center of mass,

$\beta_{\pi\pi}$ = pion velocity (in units of c) in the normal $K_S \to \pi^+\pi^-$ decay,

β = pion velocity (in units of c) in the $\pi\pi$ center of mass for the $K_S \to \pi^+\pi^-\gamma$ decay,

$\Gamma(K_S \to \pi^+\pi^-)$ = decay rate for K_S into $\pi^+\pi^-$.

Using a simulation of $\pi\pi\gamma$ decays generated according to the distribution in Eq. (29) by program FAKE,[22] we estimate that the $\pi\pi\gamma$ decays passing the selection criteria in the previous section will contribute to the time distribution

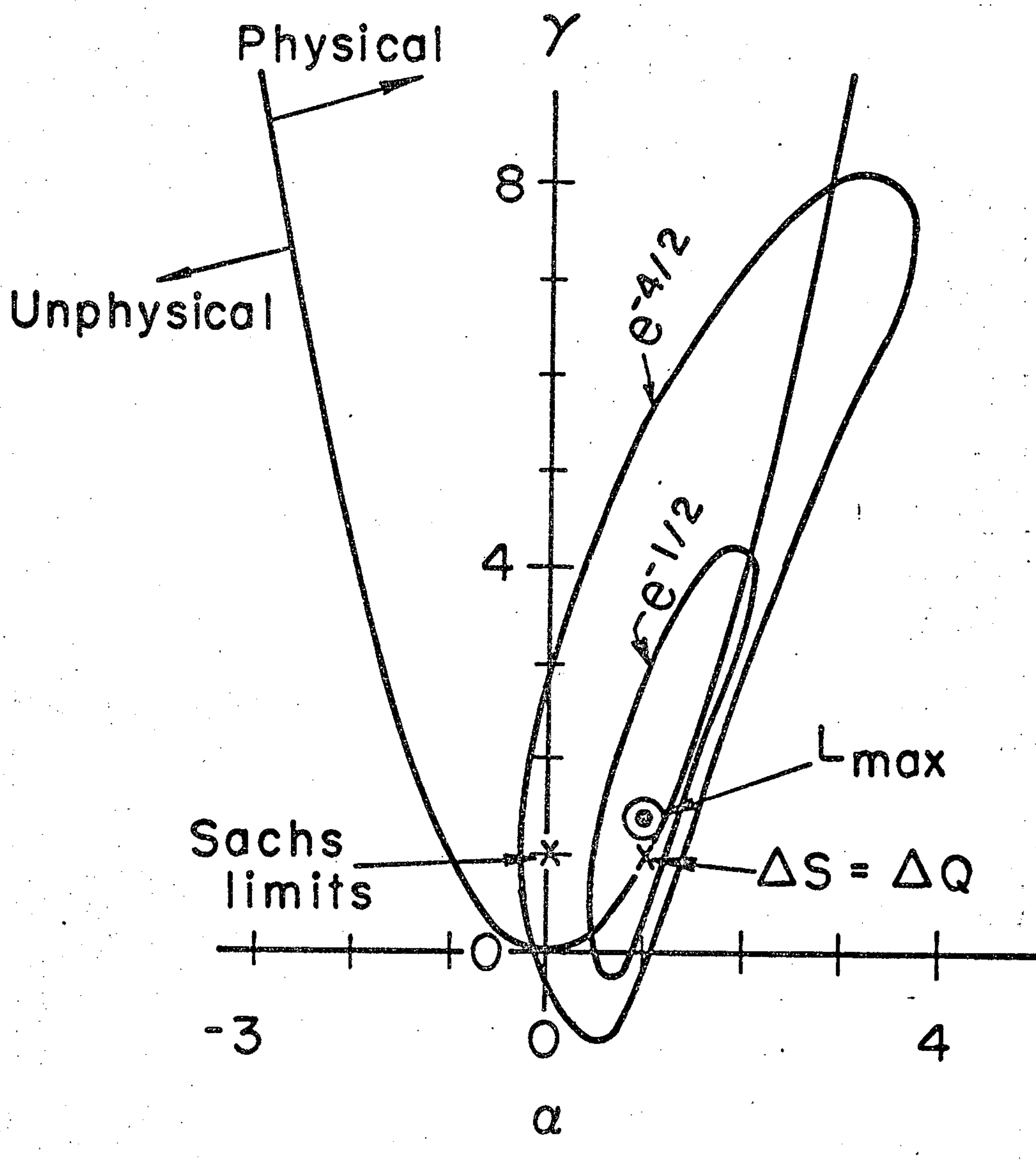

Fig. 4. Likelihood contours of α and γ on the basis of 31 events with known lepton charge (using $\Delta M = 0.75 \times 10^{10}$/sec and assuming $\beta \equiv 0$). The maximum occurs at $\gamma = 1.4^{+1.4}_{-0.9}$, $\alpha = 1.0^{+0.3}_{-0.5}$. The $\Delta S = \Delta Q$ prediction is $\gamma = 1.0$, $\alpha = 1.0$.

$$\left(\frac{dN}{dt}\right)_{\pi\pi\gamma} = 7.12\times 10^{6}\cdot \frac{N_0}{2}\exp(-\lambda_S t) \quad . \tag{30}$$

C. Analysis of the 54-Event Time Distribution

The time distribution of the 54 observed decays contains contributions from the leptonic decays (with leptons of both + and - charge) and $\pi\pi\gamma$ decays. Adding the leptonic-decay and $\pi\pi\gamma$-decay contributions (given in Eqs. 12 and 30, respectively) gives

$$\begin{aligned}\frac{dN}{dt} &= \left(\frac{dN}{dt}\right)_{leptonic} + \left(\frac{dN}{dt}\right)_{\pi\pi\gamma} \\ &= \frac{N_0\Gamma_L}{2}[1+\gamma\exp(-\lambda_S t)-2\beta\sin\Delta mt\exp(-\lambda_S t/2)] + \\ &\quad \frac{N_0}{2}\cdot 7.12\times 10^{6}\exp(-\lambda_S t)\,.\end{aligned} \tag{31}$$

Regrouping terms, we write this as

$$\frac{dN}{dt} = \frac{N_0\Gamma_L}{2}\left[1+\left(\gamma+\frac{7.12\times 10^{6}}{\Gamma_L}\right)\exp(-\lambda_S t)-2\beta\sin\Delta mt\exp(-\lambda_S t/2)\right] \tag{32}$$

Assuming that the error in γ will be relatively large, we can use any reasonable value of Γ_L to estimate the $\pi\pi\gamma$ term. We use $\Gamma_L = 12.4\times 10^{6}/\text{sec}$ (from Trilling,[10] obtained by the $\Delta I = 1/2$ prediction $\Gamma_L = 2(\Gamma_+)$) to get

$$\frac{dN}{dt} = \frac{N_0\Gamma_L}{2}[1+(\gamma+0.6)\exp(-\lambda_S t)-2\beta\exp(-\lambda_S t/2)\sin\Delta mt]\,. \tag{33}$$

We thus have a likelihood function

$$\mathcal{L}(z,\beta) = \prod_{54\ \text{events}} \frac{1+Z\exp(-\lambda_S t_i)-2\beta\exp(-\lambda_S t_i/2)\sin\Delta mt_i}{\int_{h_i}^{w_i}[1+Z\exp(-\lambda_S t)-2\beta\exp(-\lambda_S t/2)\sin\Delta mt]\,dt}, \tag{34}$$

where $Z = \gamma+0.6$.

We have calculated the likelihood for three values of Δm:

Δm	$Z\ (=\gamma + 0.6)$	β
$0.54\ \lambda_S = 0.60\times 10^{10}/\text{sec}$	-0.1	-0.6
$0.66\ \lambda_S = 0.75\times 10^{10}/\text{sec}$	$-0.7^{+1.2}_{-0.8}$	$-0.8^{+0.5}_{-0.7}$
$0.79\ \lambda_S = 0.90\times 10^{10}/\text{sec}$	-1.15	-1.2

In Fig. 5 we have displayed the likelihood contours as a function of Z and β, assuming $\Delta m = 0.75\times 10^{10}/\text{sec}$. The physical region is calculated in Appendix C to be $Z \geqslant \beta^2 + 0.6$. The most likely point in the physical region is $Z = 0.7$, $\beta = -0.3$, and the likelihood at that point is lower than the maximum by a factor of $e^{-0.35}$. The point corresponding to the predictions of $\Delta S = \Delta Q$ has a likelihood that is less than the maximum likelihood by $e^{-0.6}$.

Note that in Fig. 5 the range of possible values of β is quite large. The predictions of Sachs, that $\gamma = 1$ and $\beta = +1$ or -1, have likelihoods of $e^{-2.0}$ and $e^{-2.4}$ less than the maximum. However, substantial T asymmetries are within the $e^{-0.5}$ contour. For example, if $a_+ = 1, a_- = (-1/\sqrt{2})(1+i)$ (independent of spins, momenta, and lepton type), $\gamma = 0.2$, and $\beta = -0.4$, which is well within the $e^{-0.5}$ contour.

If we assume T symmetry (i.e., $\beta = 0$), then we measure (assuming $\Delta m = 0.75\times 10^{10}/\text{sec}$) $Z = 0.7^{+1.3}_{-1.1}$ (i.e., $\gamma = 0.1^{+1.3}_{-1.1}$).

D. Decay Rates

We first consider the measurement of Γ_L, using the non-Alexander film. In order to determine Γ_L from the 34 new events we use a modified form of Eq. (12). Suppose that a fraction g of real leptons survives the selection criteria in the Experiment section. Then in an infinite bubble chamber we would have

$$\left(\frac{dN}{dt}\right)_{\text{observed}} = g\left(\frac{dN}{dt}\right)_{\text{leptonic}} + \left(\frac{dN}{dt}\right)_{\pi\pi\gamma} . \qquad (35)$$

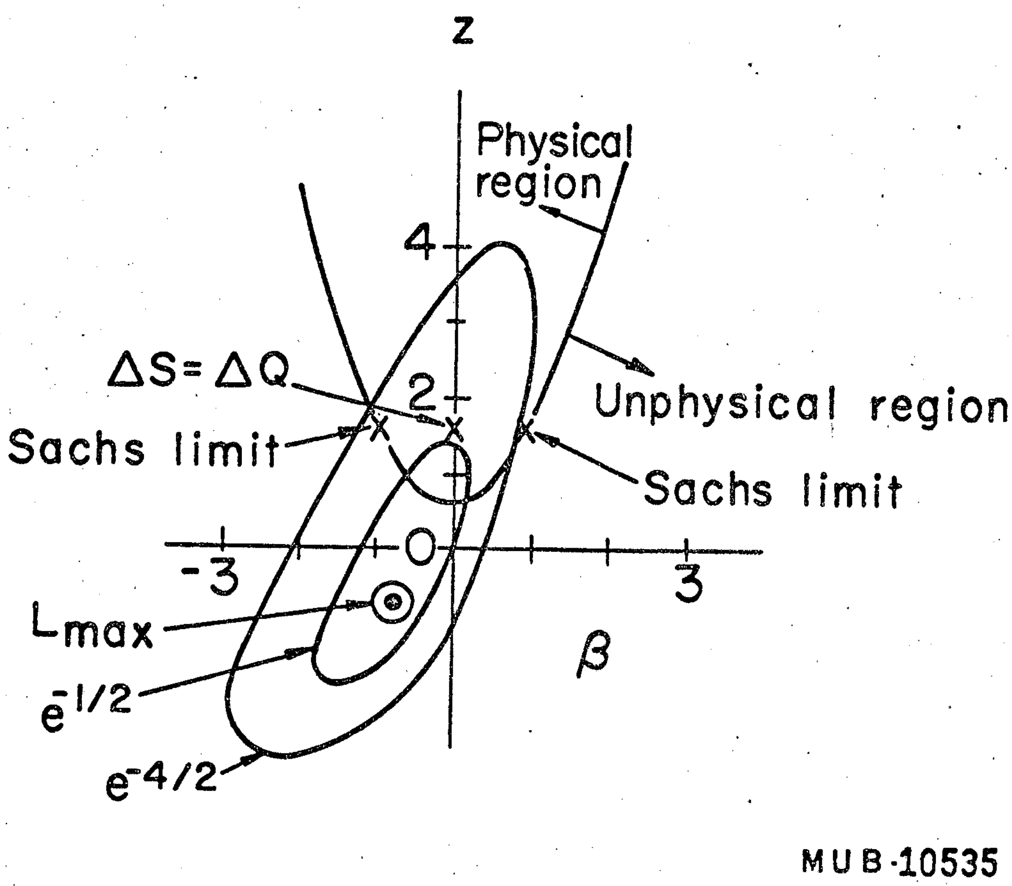

Fig. 5. Likelihood contours of Z and β on the basis of 54 events and assuming $\Delta M = 0.75 \times 10^{10}$/sec. We measure $Z = -0.7^{+1.2}_{-0.8}$, $\beta = 0.8^{+0.5}_{-0.7}$. The prediction of $\Delta S = \Delta Q$ when corrected for the $\pi\pi\gamma$ background is Z = 1.6, β = 0.

Remember that the $(dN/dt)_{\pi\pi\gamma}$ given by Eq. (30) already includes corrections for $\pi\pi\gamma$ decays lost by the cutoffs. Now, what is $(dN/dt)_{\text{leptonic}}$ for a finite bubble chamber? Well, for any particular K production it is

$$\frac{\Gamma_L}{2}[1+\gamma\exp(-\lambda_S t) - 2\beta\exp(-\lambda_S t/2)\sin\Delta m t]\,\eta(t) \tag{36}$$

where $\eta(t) = 1$ if t is less than the escape time W,
$= 0$ if t is greater than W.

So, summing up the contributions of all the K's in the experiment gives

$$\left(\frac{dN}{dt}\right)_{\text{leptonic}} = \sum_{\text{all } K^0} \frac{\Gamma_L}{2}[1+\gamma\exp(-\lambda_S t) - 2\beta\exp(-\lambda_S t/2)\sin\Delta m t]\,\eta_i(t). \tag{37}$$

Note that by $\sum_{\text{all } K^0}$ we mean sum over all K^0 whether or not the K decay is visible. This means each of the 3841 reactions $\pi^- p \to \Lambda K$, $\Lambda \to p\pi^-$ (in the non-Alexander film) is used in the sum. In a similar manner the $(dN/dt)_{\pi\pi\gamma}$ contribution is

$$\left(\frac{dN}{dt}\right)_{\pi\pi\gamma} = \sum_{\text{all } K^0} \frac{7.12\times 10^6}{2}\exp(-\lambda_S t)\,\eta_i(t)\,. \tag{38}$$

Thus

$$\left(\frac{dN}{dt}\right)_{\text{observed}} = \frac{g\,\Gamma_L}{2}\sum_{\text{all } K^0}[1+\gamma\exp(-\lambda_S t) - 2\beta\exp(-\lambda_S t/2)\sin\Delta m t]\,\eta_i(t) + \frac{7.12\times 10^6}{2}\sum_{\text{all } K^0}\exp(-\lambda_S t)\,\eta_i(t). \tag{39}$$

Integrating the above equation over all time and using

$$N_{\text{observed}} = \int_0^\infty \left(\frac{dN}{dt}\right) dt = 34 \text{ gives}$$

$$N_{\text{observed}} = \frac{g\,\Gamma_L}{2}\sum_{\text{all } K^0}\int_0^\infty [1+\gamma\exp(-\lambda_S t) - 2\beta\exp(-\lambda_S t/2)\sin\Delta n t]\,\eta_i(t)\,dt + \frac{7.12\times 10^6}{2}\sum_{\text{all } K^0}\int_0^\infty \exp(-\lambda_S t)\,\eta_i(t)\,dt \tag{40}$$

Solving for Γ_L and using the definition of η, we find

$$\Gamma_L = \frac{2\left[N_{observed} - \frac{7.12\times 10^6}{2} \sum_{\text{all } K^0} \int_0^{w_i} \exp(-\lambda_S t)\, dt\right]}{g \sum_{\text{all } K^0} \int_0^{w_i} \left[1+\lambda \exp(-\lambda_S t) - 2\beta \sin\Delta m t \exp(-\lambda_S t/2)\right] dt} \tag{41}$$

The factor g is estimated to be (89.7 ± 2.7)% by using FAKE-generated leptonic decays whose momenta are distributed according to V-A theory.[24] Performing the sums in Eq. (41) we find

$$\Gamma_L = \frac{2[34 - 2.56]}{0.897\,[5.42 + 0.36\,\gamma - 0.70\,\beta]} \times 10^6/\text{sec}. \tag{42}$$

Using the maximum-likelihood values $\gamma = -1.3^{+1.2}_{-0.8}$ and $\beta = -0.8^{+0.5}_{-0.7}$, we find $\Gamma_L = (12.5 \pm 2.7)\times 10^6/\text{sec}$. If we assume $\Delta S = \Delta Q (\gamma = 1, \beta = 0)$, we find $\Gamma_L = (12.2 \pm 2.1)\times 10^6/\text{sec}$.

Alexander et al. measure Γ_L by a similar means except they use only events beyond 3.44×10^{-10} sec, and they assume T invariance (i. e., $\beta \equiv 0$). The measured value from their events is $(10.0 \pm 2.8)\times 10^6/\text{sec}$.[27] Folding the result, $(12.5 \pm 2.7)\times 10^6/\text{sec}$ with the Alexander et al. result gives $\Gamma_L = (11.3 \pm 1.9)\times 10^6/\text{sec}$. Trilling[10] gives $\Gamma_+ = (6.2 \pm 0.35)\times 10^6/\text{sec}$, so the prediction according to $\Delta I = 1/2$ that $\Gamma_L = 2\Gamma_+ = (12.4 \pm 0.7)\times 10^6/\text{sec}$ is in good agreement with our measured value.

In Fig. 6 we display the time distribution of the 54-event sample and two smooth curves; one corresponds to $\Delta I = 1/2$[28] and the other corresponds to a completely flat decay rate.[29]

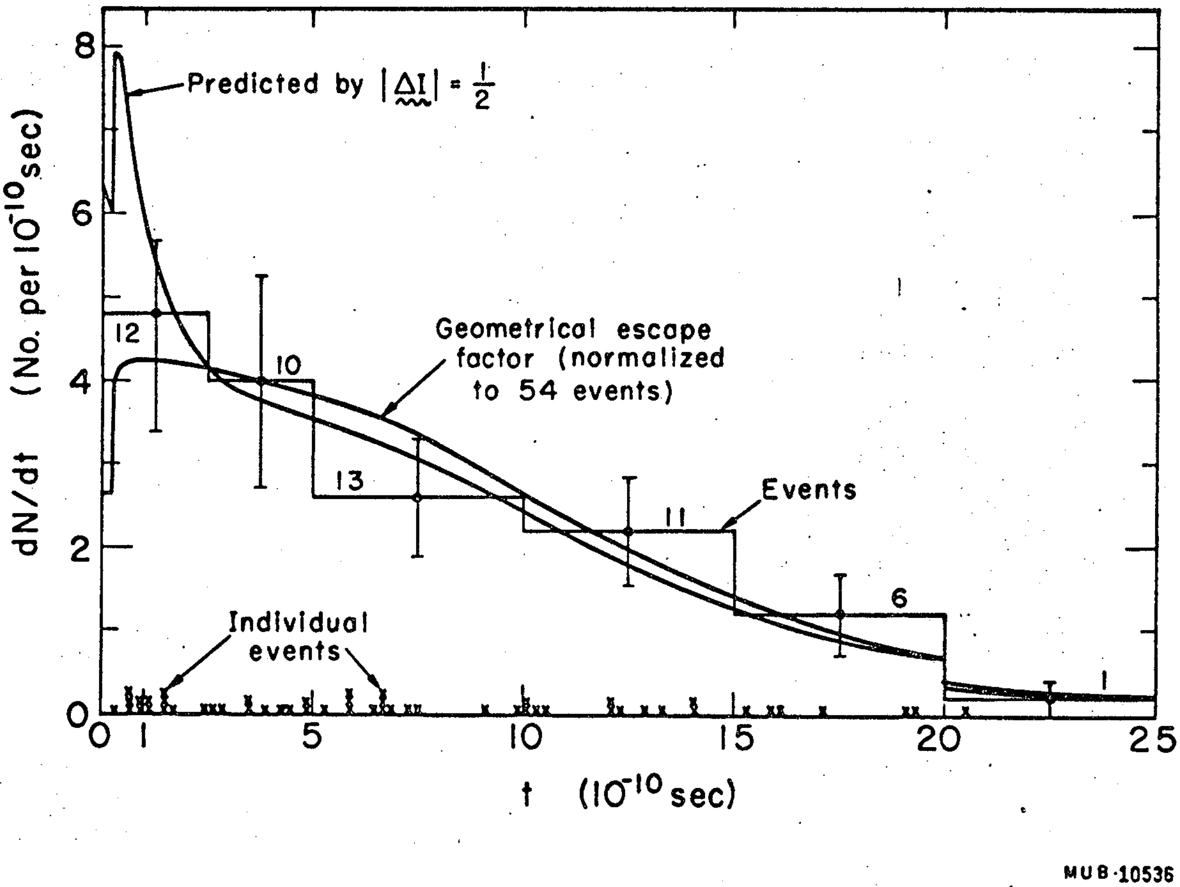

Fig. 6. Time distribution of the 54 events. The discontinuities in the theoretical curves are due to time-dependent selection criteria used in roughly a third of the film. There is one event off scale at 28.4×10^{-10} sec.

V. Discussion

The analysis of our 54 leptonic decays does not indicate any violation of the $\Delta S = \Delta Q$ rule; however, the uncertainties in our results are large enough to permit $\Delta S = \Delta Q$ amplitudes comparable in size to the $\Delta S = \Delta Q$ amplitudes. The situation of T nonconservation is quite similar. Although we find results compatible with T invariance, we cannot rule out substantial T-nonconserving amplitudes.

The measured value for the K_L leptonic decay rate is $\Gamma_L = (11.3 \pm 1.9) \times 10^6/\text{sec}$. The $\Delta I = 1/2$ prediction $(12.4 \pm 0.7) \times 10^6/\text{sec}$ obtained from the K^+ leptonic decays is in good agreement with our result. It is important to note that the prediction of the $\Delta I = 1/2$ rule used to be $\Gamma_L = (16.5 \pm 1.18) \times 10^6/\text{sec}$.[1] This would have been in serious disagreement with our measured value. However, more recent measurements of the K^+ three-body leptonic decay rates give the predicted value $(12.4 \pm 0.7) \times 10^6/\text{sec}$, which agrees well with the observed value. If one assumes that there is a $\Delta I = 3/2$, $\Delta I_z = 1/2$ amplitude a_{31} which is T-invariant (i.e., real), and that the (3/2, 3/2) amplitude is zero, then the ratio of a_{31} to the $\Delta I = 1/2$ amplitude is given by $a_{31}/a_{11} = (1/\sqrt{2})[(2\Gamma_+/\Gamma_L) - 1.0]$ (in the approximation $a_{31}/a_{11} << 1$). Thus, using $2\Gamma_+ = (12.4 \pm 0.7) \times 10^6/\text{sec}$ and $\Gamma_L = (11.3 \pm 1.9) \times 10^6/\text{sec}$, we find $a_{31}/a_{11} = 0.07 \pm 0.13$. We can then conclude with 95% confidence that $a_{31}/a_{11} < 0.33$.

ACKNOWLEDGMENTS

It is a pleasure to thank Professor Luis Alvarez and Professor Frank S. Crawford, Jr., for their guidance and encouragement. They have taught me many things about physics that one does not find in a textbook. I will always be grateful to them.

I am indebted to so many people in the Alvarez Group that I regrettably cannot name them all. However, I must thank individually all those whose contribution was crucial to the completion of the experiment. Dr. Jared A. Anderson and Mr. L. J. Lloyd, Jr., helped build the beam and organized and operated the data-reduction system for the normal events. Mr. Nick Speed, Mr. Tom Strong, and Mr. Alex Emerson did much of the difficult measuring and scan-table work necessary for selection of the lepton candidates. Dr. Don Stern wrote the kinematic analysis routines for the leptonic decays and provided many useful ideas for selection of the events. Mrs. Ann McLellan and Miss Karlyn Shepler provided secretarial assistance.

I am most thankful to my wife, Maurine, who cheerfully accepted my long hours at work and provided invaluable encouragment, financial aid, and logistical support.

This work was done under auspices of the U. S. Atomic Energy Commission.

Appendices

A. Some Invariance Properties of the Decay Amplitude

We begin by examining some of the implications of time-reversal invariance. Consider the decay $K^0 \rightarrow \pi^- e^+ \nu$. The final state consists of three particles, two of which have spin 1/2. We will specify the spin states by giving the helicities of the particles with spin. We will picture the reaction in momentum space, the origin $p_x = p_y = p_z = 0$ being chosen as the position of the K^0. The helicity of a particle will be denoted by an arrow along or against the line of flight. A typical reaction $K^0 \rightarrow \pi^- e^+ \nu$ might look like the one pictured below.

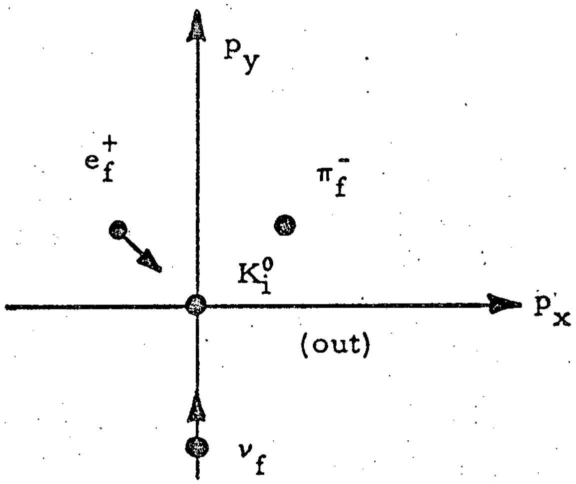

Note that we have chosen p_x and p_y to be in the decay plane. The i and f denote initial- and final-state particles, and the word "out" means the π, e, and ν have outgoing wave functions. The amplitude for the process in the first picture is $a_+(K^0 \rightarrow \pi^- e^+ \nu,\ p_\pi, p_e, p_\nu, h_e, h_\nu) = \langle \pi^- e^+ \nu,\ \text{out},\ p_\pi, p_e, p_\nu, h_e, h_\nu \mid H \mid K^0 \rangle$.

Now let's construct the time-reversed process. The time-reversed process is obtained by reversing all momenta (but not the helicities) and interchanging initial and final states.

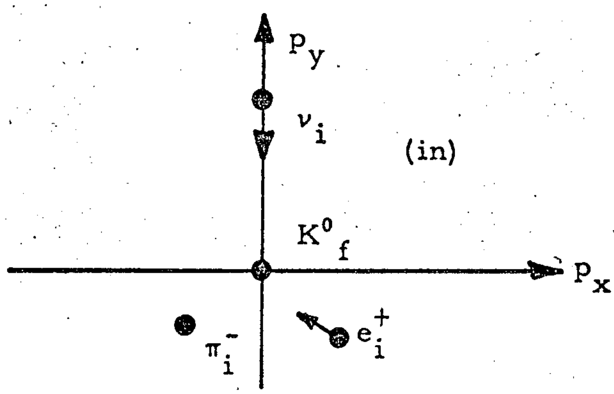

The "in" refers to the fact that the π^-, e^+, and ν are incoming. We will label this process with amplitude b_+. Thus b_+ is the amplitude for the time-reverse of the process with amplitude a_+. This process is not easily observed, but it can be related to a process we can observe. The initial and final-state labels in the time-reversed diagram can be interchanged by complex conjugation of b_+ (remember $\langle \Psi_i | H | \Psi_f \rangle = \langle \Psi_f | H | \Psi_i \rangle^*$). So the process below has amplitude b_+^*.

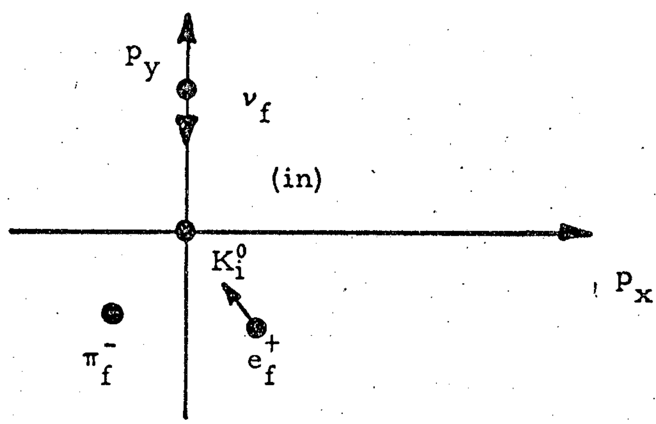

Since the decay amplitude should be rotationally invariant, the process below should also have an amplitude b_+^*.

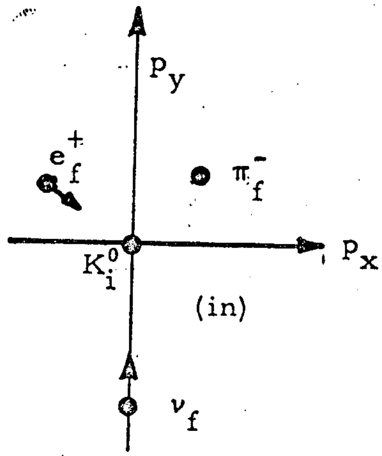

The process pictured above is a K^0 decaying to an incoming $\pi^- e^+ \nu$ system. This is not an observable final state. The incoming waves will scatter and become outgoing waves introducing a phase shift $e^{i\delta}$ into the reaction amplitude. However, since there is only one nuclear particle in the final state, the scattering is only electromagnetic. Consequently the phase shift should be negligible. Thus the process pictured below should have an amplitude b_+^*.

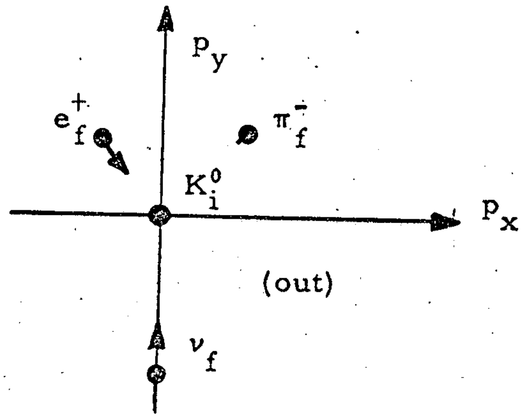

But this process is the same process as in the first picture. Since this process has amplitude a_+ we must conclude that $b_+^* = a_+$. Thus $b_+ = a_+^*$. So, given a leptonic decay with amplitude a_+, the time-reverse of this process has amplitude a_+^*. Time-reversal invariance requires that a process and its time reverse have the <u>same</u> amplitude, thus time-reversal invariance demands that a_+ be real. Similarly, time-reversal invariance requires that the amplitude a_- (for $K^0 \to \pi^+ e^- \nu$) be real.

Now we turn to a discussion of the consequences of the CPT theorem. Consider the decay $K^0 \rightarrow \pi^+ e^+ \nu$ again (remember the amplitude is a_+). We will apply the T, P, and C transformations to the process and find a new process whose amplitude is a_+ (provided the CPT theorem is valid). We begin by picturing our initial process again.

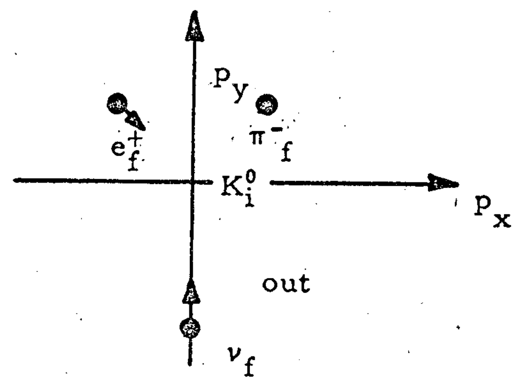

Next we apply the time-reversal operator (in the same manner as in the previous section). The time-reversed process is pictured below.

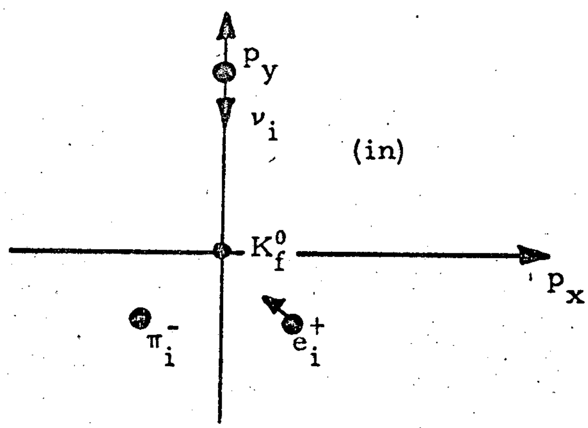

The parity operator P reverses the momenta but not the helicities:

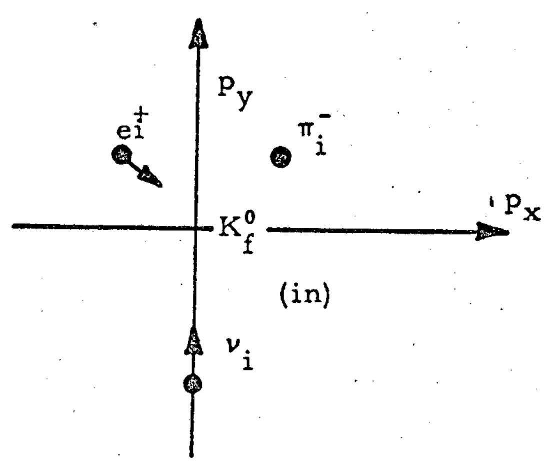

The charge-conjugation operator changes each particle to its anti-particle and reverses the helicities:

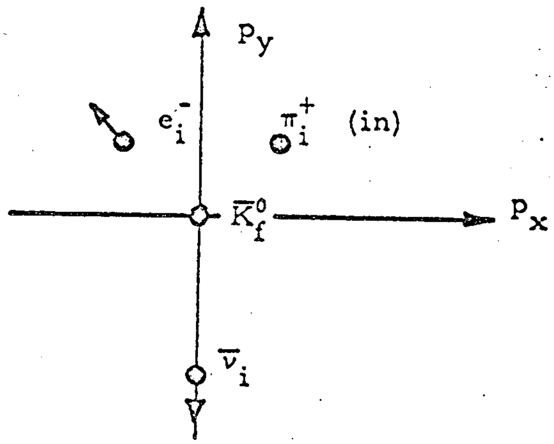

The CPT theorem says this process must have amplitude a_+. Note that the process pictured above is not physically observable. Just as in the previous paragraphs on time-reversal invariance, we can interchange initial and final states, obtaining a new state with amplitude a_+^*.

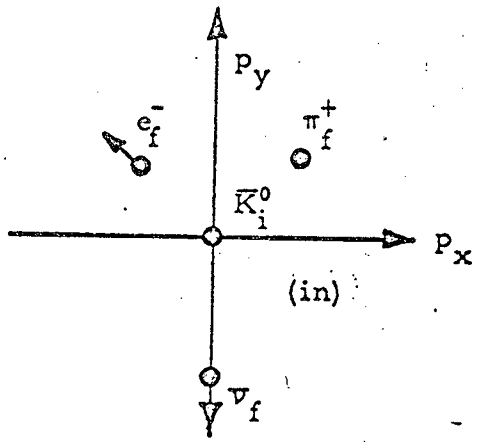

Next, we allow the $e^-\pi^+$ and ν waves to scatter and become outgoing waves.

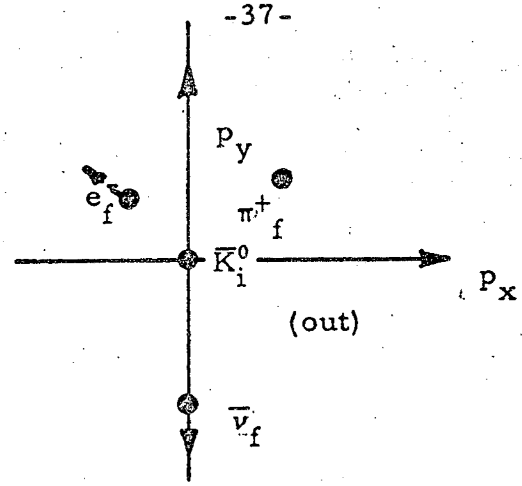

The process pictured above is one of those we are studying. We now know that it has amplitude a_+^*. Note that the helicities are not the same as in the original process. We ignore this minor detail in the main text because we eventually average over spin.

In conclusion, we have found that, if the process $K^0 \to \pi^- e^+ \nu$ has an amplitude $a_+ (p_\pi, p_e, p_\nu, h_e, h_\nu)$, then the process $\overline{K}^0 \to \pi^+ e \nu$ with the same momenta but opposite helicities has an amplitude $a_+^* (p_\pi, p_e, p_\nu, h_e, h_\nu)$. Similarly, if the process $K^0 \to \pi^+ e^- \nu$ has amplitude $a_- (p_\pi, p_e, p_\nu, h_e, h_\nu)$, then the process $\overline{K}^0 \to \pi^- e^+ \nu$ at the same momenta but opposite helicities has amplitude $a_-^* (p_\pi, p_e, p_\nu, h_e, h_\nu)$.

B. The $p\beta\Delta\theta$ Cutoff

Coulomb scattering is predominantly small angle. To calculate the cutoff we examine the Rutherford cross section as a function of $p\beta\Delta\theta$ and ask that for the 2500 K decays in the experiment less than 0.3 of them have a scatter with a $p\beta\Delta\theta$ greater than our cutoff. Suppose a particle with velocity v scatters from a proton with an impact parameter b. The scattering angle for the incident particle is[30]

$$\Delta \theta \approx \frac{\Delta p}{p} = \frac{F \Delta t}{p} = \frac{\left(\frac{e^2}{b^2}\right)\left(\frac{2b}{v}\right)}{p} = \frac{2\, e^2}{p\, b\, v}, \tag{43}$$

therefore, solving for b, using $v = \beta c$, we find

$$b = \frac{2e^2}{p\beta\Delta\theta c} \quad . \tag{44}$$

To get into more convenient units put p in MeV/c [use $\frac{1}{3}\times 10^4\, p\,(\text{MeV}/c) = \frac{Pc}{e}$ (CGS)] and convert $\Delta\theta$ to degrees. This gives

$$b = \frac{1.6\times 10^{-11}}{p\beta\Delta\theta} \text{ cm.} \tag{45}$$

The cross section for $\Delta\theta$ larger than $\Delta\theta_0$ (and hence $p\beta\Delta\theta$ larger than $p\beta\Delta\theta_0$) is

$$\sigma = \pi b^2 = \pi \left(\frac{1.6\times 10^{-11}}{p\beta\Delta\theta_0}\right)^2 . \tag{46}$$

Note that σ falls off with increasing $p\beta\Delta\theta_0$. We want to pick a cutoff $p\beta\Delta\theta_0$ large enough to make the cross section so small that only 0.3 event can exceed $p\beta\Delta\theta_0$. The number A of scatterings with $p\beta\Delta\theta \geqslant p\beta\Delta\theta_0$ produced from N K decays, each with an average track length x, is

$$A = (\eta x\ \sigma\ N)\cdot 2 = 2\,\eta\, x\, N\, \pi \left(\frac{1.6\times 10^{-11}}{p\beta\Delta\theta_0}\right)^2 , \tag{47}$$

where the factor of 2 is because there are two tracks for each K decay, and η is the number of scattering centers per cc $\approx 0.3\times 10^{23}$. Solving for $p\beta\Delta\theta_0$,

$$p\beta\Delta\theta_0 = \sqrt{\frac{2\pi\,\eta\, x\, N\cdot (1.6\times 10^{-11})^2}{A}} , \tag{48}$$

we find, for A = 0.3, x=20 cm, and N = 2500,

$$p\beta\Delta\theta_0 = 2900\,\frac{\text{MeV deg}}{c} . \tag{49}$$

The average scattering takes place in the middle of the track, thus the angle of the track at its beginning as reconstructed from the measurement will be shifted by $\approx \frac{1}{2}$ the scattering angle. When the fit $K_S \to \pi^+\pi^-$ is performed we assume that the fitted angle for the deleted track is the unscattered track angle. Thus the angle of the scattering is $2\,|\theta_{fit} - \theta_{meas}|$. Therefore, if we use $2|\theta_{fit} - \theta_{meas}|$ instead of $\Delta\theta_0$, genuine Coulomb scatterings would satisfy

$$p\beta\,|\theta_{fit} - \theta_{meas}| \equiv p\beta\Delta\theta \leqslant 1450\ \frac{\text{MeV deg}}{c} . \tag{50}$$

We use only events for which

$$p\beta\Delta\theta \geqslant 2000\frac{\text{MeV deg}}{c} . \tag{51}$$

This assures us that they are not Coulomb scatterings.

C. Techniques for Particle Identification

As noted in the introduction, the identification of the lepton charge can be of great value. In principal, the lepton in a K leptonic decay could always be identified by momentum and energy conservation. However, momentum uncertainties which give rise energy uncertainties comparable to the mass differences between π and μ and e are frequent. This leads to the situation of ambiguous events, that is, events which satisfy energy and momentum conservation equally well for several fitting hypotheses. In our experiment the few events which were kinematically unambiguous were of the type $K \rightarrow \pi^+ e^- \nu$. and $K \rightarrow \pi^- e^+ \nu$.

Realizing the difficulty in charge identification by kinematics, we have made a serious attempt to utilize the techniques outlined below.

1. Ionization

Consider Rutherford scattering at a fixed impact parameter. The momentum transfer to the target is $\Delta p = F\Delta t$, where F is the average force and Δt is the time duration of the collision. Since the force does not depend on the velocity, the momentum transfer is proportional to Δt and thus inversely proportional to β. Therefore the energy transfer is $1/\beta^2$.

This simple-minded approach indicates that particles will lose energy according to

$$\frac{dE}{dx} = \left(\frac{dE}{dx}\right)_{\beta=1} \cdot \frac{1}{\beta^2} . \tag{52}$$

For hydrogen bubble chambers this form has been verified experimentally by Fabian et al.[31] The technique used to measure dE/dx is to measure the average gap between bubbles. If one assumes that each bubble represents a certain amount of deposited energy ΔE, then $dE/dx = \Delta E/\Delta G$, where ΔG is the average bubble gap. The β of a particle is measured by measuring ΔG for the particle and for another nearby particle whose momentum is high enough to guarantee $\beta \approx 1$. Then

$$\frac{1}{\beta^2} = \frac{\Delta G\,(\text{fast particle})}{\Delta G\,(\text{particle of interest})} = 1 + \left(\frac{m}{p}\right)^2 . \tag{53}$$

The momentum of the particle is known by measuring its curvature, so, since β and p are known, the mass can be determined.

It is not always possible to measure ΔG accurately. Even with a good microscope, when the average gap space as seen in the best camera view is $\approx 1/2$ that of a fast particle it becomes difficult to separate the bubbles. The gaps are measured in a particular view, and the measurements must be corrected for the projection angle between the track and the viewing camera. A gap is measured only if the two bubbles can be easily distinguished.

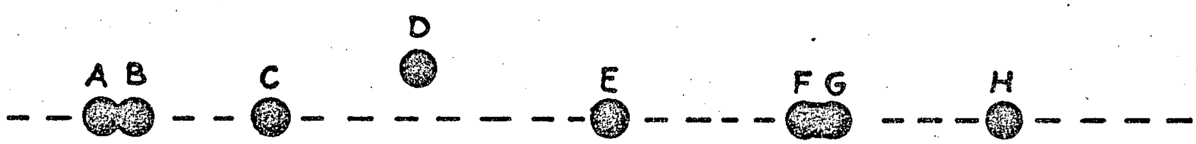

A gap is not measured unless the bubble overlaps the line of flight. In the sketch of a track (above) the gaps AB, BC, CE, EF, and GH would be measured but CD, DE and FG would not be.

Obviously there is a bias against small gaps. To measure the average gap from the biased sample we use the fact that the bubbles are created independently, and therefore the gaps are exponentially distributed with a slope (on semilog paper) of ΔG. Thus the short gaps are not essential. The ionization technique is accurate enough to distinguish an electron from a pion when the track momentum is less than ≈ 180 MeV/c, provided the track is approximately perpendicular to the viewing axis. Therefore only the relatively low-momentum tracks can be analyzed with this technique. For very-low-momentum tracks it is not necessary to count the bubble gaps; for tracks of momentum less than ≈ 100 MeV an electron can be easily distinguished from a pion on the scanning table, but again, the track must be roughly perpendicular to the viewing axis. If any hypothesis in this work predicted an ionization more than three standard deviations from the measured value, the hypothesis was regarded as invalid.

2. δ Rays

In principle, of a track of known momentum scatters an electron with enough momentum transfer to make the recoil electron momentum measurable, the scattering vertex can be fitted and the mass of the track determined. This technique is discussed in great detail by Crawford.[32] A simplfied version was used for the leptonic decay experiment. The technique is based on the fact that a large δ ray almost always signifies that the primary track was an electron.

The maximum kinetic energy δ ray is produced by a head-on scattering. Its energy can be calculated easily by transforming the target four-momentum into the collision center-of-mass. Assuming the motion is in the +x direction, we have

$$(0, 0, 0, m_e) \xrightarrow{\text{Lorentz}} (-\eta m_e, 0, 0, \gamma m_e) \tag{54}$$

where $\eta = \dfrac{\text{momentum of incident track} \equiv p}{\text{Invariant mass of system} \equiv \mu}$,

$\gamma = \eta^2 + 1.$

After the collision the target four-momentum is

$$(+\eta\, m_e, 0, 0, \gamma\, m_e). \tag{55}$$

The fourth component, in the laboratory system, is

$$E_e = T_e + m_e = \eta^2 m_e + \gamma^2 m_e, \tag{56}$$

so the max kinetic energy T_e is

$$T_e = (\eta^2 + \gamma^2 - 1)\, m_e. \tag{57}$$

But $\gamma^2 - 1 = \eta^2$, so

$$T_e = 2\eta^2 m_e = \frac{2p^2 m_e}{\mu^2} \quad . \tag{58}$$

The invariant mass squared is

$$\mu^2 = m^2 + m_e^2 + 2\sqrt{m^2 + p^2}\, m_e \, , \tag{59}$$

where m is the mass of the primary track. Thus

$$T_e(\max) = \frac{2p^2 m_e}{m^2 + m_e^2 + 2\sqrt{m^2 + p^2}\, m_e} \approx P_e(\max) \, . \tag{60}$$

The value of the primary momentum p is known by measuring the curvature of the incident track.

As an example, suppose a track with p = 300 MeV/c is observed to have a 30-MeV/c δ ray. If the incident track is a π, then $P_e(\max)$ = 4.5 MeV/c; if it is a μ, then $P_e(\max)$ = 9 MeV/c; if it is an e, then $P_e(\max)$ = 300 MeV/c. Thus the δ ray of momentum larger than 9 MeV/c implies that the track is an electron.

3. Nuclear interactions

A nuclear interaction on a track from a K decay is a clear indication that the track was a pion.

The nuclear interaction typically appears in two forms, one form being a two-prong configuration, for example,

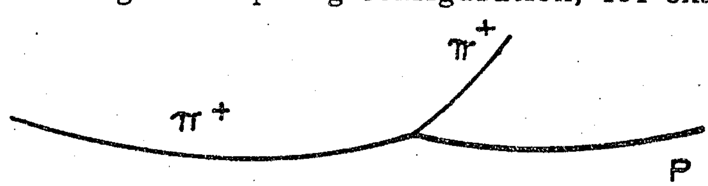

and the other form a zero-prong configuration, for example

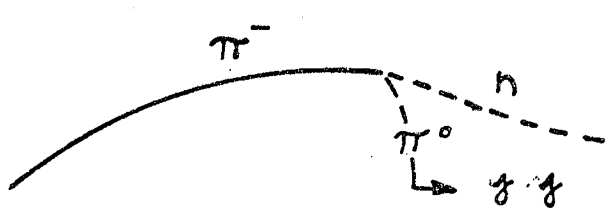

The latter process almost always occurs on slow π^- tracks, and is characterized by a slow, heavily ionizing negative track that terminates abruptly in the chamber.

It should be pointed out that for events that fit $\pi\pi\gamma$ as well as leptonic hypotheses, the identification of one track as a pion does not imply that the other track is a lepton.

4. Decays of tracks

Occasionally a track can be identified as a pion because of a $\pi \to \mu\nu$ decay. This can be distinguished from a $\mu \to e\nu\bar{\nu}$ decay by measuring the track and its decay product and performing a 1c fit. A $\mu \to e\nu\bar{\nu}$ decay can be identified by the wide angle of the decay or by identification of the electron as the decay product.

D. Relationships between α, β and γ

Referring to the definitions of α, β and γ in Eq. (10), and recalling $\Gamma_L = \sum_l \langle |(a_+ - a_-^*)|^2 \rangle$, we have

$$\gamma = \sum_l \langle |a_+ + a_-^*|^2 \rangle / \Gamma_L ,$$

$$\alpha = \sum_l \langle \mathrm{Re}(a_+ - a_-^*)(a_+^* + a_-) \rangle / \Gamma_L , \qquad (61)$$

$$\beta = \sum_l \langle \mathrm{Im}(a_+ - a_-^*)(a_+^* + a_-) \rangle / \Gamma_L .$$

Now redefine the averaging process and the sum over lepton type to be a sum over pure states denoted by i (the states have definite momenta, spins, lepton type, etc.). Then we have

$$\gamma = \sum_i |(a_+ + a_-^*)_i|^2 / \Gamma_L , \qquad (62)$$

$$\alpha = \sum_i \mathrm{Re}(a_+ - a_-^*)_i (a_+^* + a_-)_i / \Gamma_L ,$$

$$\beta = \sum_i \mathrm{Im}(a_+ - a_-^*)_i (a_+^* + a_-)_i / \Gamma_L ,$$

and therefore

$$\alpha^2 + \beta^2 = \Big|\sum_i (a_+ - a_-^*)_i (a_+^* + a_-)_i\Big|^2 / \Gamma_L^2 \ .$$

Using a Schwartz inequality, $\Big|\sum_i A_i B_i\Big|^2 \leqslant (\sum_i |A_i|^2)(\sum_i |B_i|^2)$,

we have

$$\alpha^2 + \beta^2 \leqslant (\sum_i |(a_+ - a_-^*)_i|^2)(\sum_i |(a_+^* + a_-)_i|^2)/\Gamma_L^2 \ , \tag{63}$$

$$\alpha^2 + \beta^2 \leqslant \gamma^2 \ . \tag{64}$$

In case α is unknown the relationship reduces to

$$\beta^2 \leqslant \gamma. \tag{65}$$

This is the curve in Fig. 5. The curve in Fig. 4 is just Eq. (64) with $\beta \equiv 0$.

Table I. Observed decays.

The spaces with -- in the χ^2 columns represent hypotheses for which $\chi^2 > 20$ or for which the fitting procedure would not converge. The variables h and w are the minimum and maximum acceptance times (in the K rest system) for each event, and t is the elapsed proper time of the decay.

	Identification number	$\chi^2_{\pi\pi\gamma}$	$\chi^2_{\pi^+e^-\nu}$	$\chi^2_{\pi^+\mu^-\nu}$	$\chi^2_{\pi^-e^+\nu}$	$\chi^2_{\pi^-\mu^+\nu}$	t_0	t	t_ω	Lepton	Means of identification
1.	503063	--	4.6	--	--	--	0.20	5.90	15.16	e^-	fit and δ ray
2.	505231	--	4.2	--	--	3.1	0.20	3.45	20.00	--	
3.	521330	1.1	--	5.1	4.0	2.2	0.20	2.65	3.99	--	
4.	525293	--	13.3	3.2	14.9	2.1	0.29	12.04	13.15	--	
5.	532310	--	1.7	4.4	--	0.1	0.20	15.26	20.00	--	
6.	564390	2.2	0.0	0.7	0.0	0.7	0.20	2.87	9.42	--	
7.	565027	--	5.9	--	1.2	9.8	0.20	7.29	10.16	e^+	ionization
8.	668583	--	0.45	--	0.91	--	0.0	0.79	8.19	e^-	scatter on +
9.	692228	--	4.1	--	3.2		0.20	2.47	12.65	e^-	ionization
10.	704248	--	19.0	3.1	1.0	10.9	0.20	0.91	11.91	--	
11.	707247	1.5	5.1	0.1	0.6	0.1	0.22	1.48	2.62		
12.	713256	--	--	7.4	--	0.9	0.34	1.45	19.54	μ^+	π^- charge exch.
13.	714067	0.8	--	--	13.4	1.5	0.20	6.48	19.69		
14.	722026	2.2	--	2.0	10.6	0.5	0.20	6.79	16.24		
15.	735269	--	--	--	1.6	--	0.20	1.10	18.46	e^+	fit
16.	756453	--	0.3	8.8	--	0.3	0.30	15.94	20.00	μ^+	kinematics
17.	774147	--	6.0	--	0.0	15.3	0.21	13.36	18.96	e^+	ionization
18.	781181	--	--	2.1	--	2.2	0.23	3.84	12.51	μ^-	decay
19.	781208	1.9	4.7	0.0	0.0	0.6	0.20	0.36	20.00	--	
20.	819009	9.6	3.7	0.4	6.7	0.1	0.20	6.97	20.00	--	
21.	844335	--	0.0	--	16.6	2.4	0.20	17.16	20.00	e^-	δ ray
22.	1370287	--	18.3	--	0.52	--	0.00	0.72	9.99	e^+	fit
23.	1376303	--	--	1.2	1.0	--	0.00	5.85	8.75	μ^-	decay on -
24.	1411172	--	1.58	9.9	3.3	8.7	0.00	0.96	7.51	e^+	δ ray on +
25.	1432236	--	--	--	1.06	--	0.00	1.78	11.51	e^+	fit
26.	1449151	--	0.005	--	--	--	0.00	10.38	18.14	e^-	fit
27.	1460602	--	--	--	4.9	--	0.00	9.19	10.24	e^+	fit

Table I. (Continued)

	Identification number	$\chi^2_{\pi\pi\gamma}$	$\chi^2_{\pi^+e^-\nu}$	$\chi^2_{\pi^+\mu^-\nu}$	$\chi^2_{\pi^-e^+\nu}$	$\chi^2_{\pi^-\mu^+\nu}$	t_0	t	t_ω	Lepton	Means of identification
28.	1465026	--	--	--	2.2	--	0.00	1.49	6.26	e^+	fit
29.	1481269	0.005	4.45	--	15.5		0.00	5.32	16.84	--	
30.	1492562	0.47	2.5	1.3	1.4	0.9	0.00	12.32	21.24	μ^+	decay
31.	1707025	--	8.40	5.1	1.6	--	0.00	10.41	15.82	e^-	ionization
32.	1714542	--	6.9	--	--	--	0.00	4.36	10.61	e^-	fit and δ ray
33.	1720407	--	5.4	4.3	5.7	15.4	0.00	12.21	14.59	e^+	π μ e
34.	1720440	2.6	6.4	4.0	4.4	3.4	0.00	4.97	10.30	e^-	ionization
35.	1723585	--	4.3	--	0.28	--	0.00	5.80	8.06	e^+	ionization
36.	1739122	0.4	2.2	1.1	1.2	0.73	0.00	20.43	22.43	--	
37.	1763407	18.2	1.5	7.3	0.03	3.5	0.00	6.81	10.80	--	
38.	1781541	--	--	3.4	2.5	3.8	0.00	9.86	14.49	μ^-	ionization
39.	1782493	--	--	--	0.17	--	0.00	1.02	14.04	e^+	fit
40.	1793046	0.26	0.04	0.03	0.03	0.04	0.00	4.53	9.86	--	
41.	1800086	3.2	--	3.4	--	18.5	0.00	19.33	29.44	--	
42.	1801287	--	--	--	0.31	--	0.00	10.04	16.26	e^+	fit and δ ray
43.	1823465	0.05	0.8	0.06	6.1	0.79	0.00	19.19	24.41	--	
44.	1830604	--	--	--	0.41	--	0.00	16.01	17.36	e^+	fit
45.	1831602	1.6	10.6	1.0	0.99	0.03	0.00	0.79	8.15	--	
46.	1834228	0.69	2.3	0.04	1.3	0.0005	0.00	12.92	18.96	--	
47.	1834229	--	1.1	10.7	0.05	4.8	0.00	3.53	21.61	--	
48.	1835104	--	0.41	--	1.5	--	0.00	7.45	20.18	e^-	ionization
49.	1835387	--	0.003	8.3	0.75	10.1	0.00	4.95	6.97	--	
50.	1845281	--	17.9	--	2.8	--	0.00	14.06	16.50	e^+	fit
51.	1866202	7.0	0.9	3.7	0.002	2.3	0.00	6.73	17.83	e^-	δ ray
52.	1867422	1.8	6.1	2.2	3.4	0.79	0.00	28.40	35.21	--	
53.	1885046	--	--	0.75	0.83	--	0.00	10.04	15.37	e^+	charge exch. on -
54.	1898594	--	0.74	12.3	10.1	1.6	0.00	14.05	16.45	--	

REFERENCES

1. Gideon Alexander, Silverio P. Almeida, and Frank S. Crawford, Jr., Phys. Rev. Letters 9, 69 (1962).
2. Frank S. Crawford, Jr. (Lawrence Radiation Laboratory), private communication.
3. Robert A. Becker, Introduction to Theoretical Mechanics (McGraw-Hill Book Company, New York, 1954), p. 341.
4. See, for example, Gerald W. Meisner, Bevalyn B. Crawford, and Frank S. Crawford, Jr., Phys. Rev. Letters 16, 278 (1966).
5. Frank S. Crawford, Jr., Marcello Cresti, Roger Douglass, Myron L. Good, George R. Kalbfleisch, and M. Lynn Stevenson, Phys. Rev. Letters 2, 361 (1959).
6. R. P. Ely et al. (California-Padua-Wisconsin Collaboration), Phys. Rev. Letters 8, 132 (1962).
7. B. Aubert, L. Behr, J. P. Lowys, P. Mittner, and C. Pascand, Phys. Letters 10, 214 (1964).
8. M. Baldo-Ceolin, E. Calimani, S. Ciampollillo, C. Filippi-Filosofo, H. Huzita, F. Mattioli, and G. Miari, Nuovo Cimento 38, 684 (1965).
9. P. Franzini, L. Kirsch, P. Schmidt, J. Steinburger, and R. J. Plano, Phys. Rev. 140, B127 (1965).
10. George H. Trilling, K Decay, Lawrence Radiation Laboratory Report UCRL-16473, Nov. 1965. (This is a paper presented to the 1965 International Conference on Weak Interactions, Argonne National Laboratory. It summarizes present K-decay data.)
11. Frank S. Crawford, Jr., Phys. Rev. Letters 15, 1045 (1965).
12. Philippe H. Eberhard, Phys. Rev. Letters 16, 150 (1966).
13. T. D. Lee, Reinhard Oehme, and C. N. Yang, Phys. Rev. 106, 340 (1957).
14. Frank S. Crawford, Jr., Strange-Particle Decays, Lawrence Radiation Laboratory Report UCRL-10540, Nov. 1962.
15. Murray Gell-Mann and Arthur H. Rosenfeld, Ann. Rev. Nucl. Sci. 7, 407 (1957).

16. R. G. Sachs, Phys. Rev. Letters 13, 286 (1964).

17. Sanford E. Wolf, Norbert Schmitz, Lester J. Lloyd, William Laskar, Frank S. Crawford, Jr., Janice Button, Jared A. Anderson, and Gideon Alexander, Rev. Mod. Phys. 33, 439 (1961).

18. A discussion of this system and other related programs together with detailed references may be found in Arthur H. Rosenfeld, Current Performance of the Alvarez Group Data Processing System, Nucl. Instr. Methods 20, 422 (1963).

19. N. P. Samios, Phys. Rev. 121, 275 (1961).

20. Donald Stern, Thomas D. Binford, V. Gordon Lind, Jared A. Anderson, Frank S. Crawford, Jr., and Robert L. Golden, Phys. Rev. Letters 12, 459 (1964).

21. The effect of this and the other cutoffs on bona fide leptonic decays was investigated by using Monte-Carlo-generated events. The momenta were distributed according to V-A theory (Ref. 23). The events were generated by program FAKE (Ref. 22) and then tried as $\pi\pi\gamma$.

22. Gerald R. Lynch, Program FAKE. Monte Carlo Simulation of Bubble Chamber Events, Lawrence Radiation Laboratory Report UCRL-10335, July 1962.

23. We used a pure vector matrix element and assumed $\xi = 0$. D. Luers, I. S. Mittra, W. J. Willis, and S. S. Yamamoto, Phys. Rev. 133, B1276 (1964).

24. We used branching ratios given in Arthur H. Rosenfeld, Angela Barbaro-Galtieri, Walter H. Barkas, Pierre L. Bastien, Janos Kirz, and Matts Roos, Data on Particles and Resonant States, Lawrence Radiation Laboratory Report UCRL-8030 Part I, March 1965.

25. The calculation is made upon assumption of pure inner bremsstrahlung (i.e., no direct processes), and also assumption of a constant form factor for the $\pi\pi$ vertex. We now turn to a discussion of the validity of the inner-bremsstrahlung hypothesis. If CP were absolutely conserved the direct process $K_L \to \pi^+\pi^-\gamma$ would be allowed. Since CP is very nearly conserved we might

expect that the rate of the K_L direct process is larger than the direct rate for the K_S (this is of course assuming that the direct process is CP conserving). In Franzini et al. (Ref. 9) it is pointed out that an upper limit for the branching ratio for $K_L \rightarrow \pi^+\pi^-\gamma$ (by direct and final state processes) is 1%. Thus the rate for $K_S \rightarrow \pi^+\pi^-\gamma$ is probably less than $0.01\ \Gamma_L$ and therefore negligible. Experimental observation of the $K_S \rightarrow \pi^+\pi^-\gamma$ decay is exceedingly difficult because of measurement inacuracies (which make $\pi\pi\gamma$ hard to distinguish from $\pi\pi$).

26. Jonas Schultz (Lawrence Radiation Laboratory), private communication.

27. This differs slightly from the value $(9.31 \pm 2.7) \times 10^6$/sec published by Alexander et al. because of a recalculated geometrical escape correction.

28. Both the shape and the normalization correspond to $\Delta I = 1/2$. The normalization predicted from the K^+ data is 54.6 events, including an estimated 10.7% loss due to our selection criteria and including 2.56 $\pi\pi\gamma$ decays.

29. This is just the geometrical escape factor (i.e., the fraction of K^0 produced in our film that are still in the chamber at time t). It is normalized to 54 events, and is calculated on the basis of all 6544 reactions of the type $\pi^- p \rightarrow \Lambda K$, $\Lambda \rightarrow p\pi^-$ (whether or not the K decay was seen).

30. This calculation is crude but the end result is the same as doing it the hard way.

31. B. Fabian, R. Place, W. Riley, and W. Sims, Rev. Sci. Instr. 34, 484 (1963).

32. Frank S. Crawford, Jr., Alvarez Group Memo No. 106.